

Adaptive observers for biophysical neuronal circuits

Thiago B. Burghi and Rodolphe Sepulchre

Abstract—This paper presents adaptive observers for online state and parameter estimation of a class of nonlinear systems motivated by biophysical models of neuronal circuits. We first present a linear-in-the-parameters design that solves a classical recursive least-squares problem. Then, building on this simple design, we present an augmented adaptive observer for models with a nonlinearly parameterized internal dynamics, the parameters of which we interpret as structured uncertainty. We present a convergence and robustness analysis based on contraction theory, and illustrate the potential of the approach in neurophysiological applications by means of numerical simulations.

Index Terms—Adaptive observers, Nonlinear systems, Conductance-based models, Contraction theory, Neuroscience.

I. INTRODUCTION

With the development and refinement of neural recording technology, controlling the nervous system at the cellular scale may soon become possible. Techniques such as voltage imaging [21], for instance, promise to deliver simultaneous subthreshold recordings of large biological neural networks, opening up new possibilities for the design of brain-machine interfaces [35]. But while these technologies are still maturing, closed-loop control of small living neuronal circuits has been a reality since the development of the *dynamic clamp* [43] electrophysiology technique. Even though the control of such small circuits is not yet done in a systematic fashion, it has enabled important scientific discoveries related to the electrochemical process of neuromodulation [29], [33].

The systematic control of small neural circuits is an open problem [7] that will only become more challenging as the scale of the circuits is increased. The main bottleneck is the ever changing nature of living neurons [44], which implies that any model-based approach to neuronal control must consider online estimation methods. Any such estimation method should deal with the spiking nature of electrophysiological signals, and the consequent nonlinearity of state-space neuronal models [18], [20]. In particular, *conductance-based models*, introduced in the seminal work [15], have a large number of

uncertain parameters and unmeasured states, and dealing with this issue has been an important modelling challenge [14].

The question of estimating conductance-based neuronal models from input-output data has mostly been approached with *offline* algorithms and *output-error* [24] model structures, see e.g. [10], [32], [36]. However, since the neuronal dynamics lack the fading memory property that is essential for performing output-error estimation [23], [24], [27], such methods lead to difficult optimization problems with nonsmooth cost functions [1], [39]; as a consequence, the use of such methods in adaptive schemes is precluded. To deal with these difficulties, some authors have exploited the assumption that the only parameters to be estimated are a neuron's *maximal conductances* (including synaptic weights), while other parameters related to ion channel properties can be assumed known. In this case, the neuronal model structure becomes linear-in-the-parameters [4], [17], [34]. An important question related to such approaches is the effect of ion channel model uncertainty.

In this paper, we address the problem of *online* estimation of single-neuron and neural network conductance-based models. Our modelling framework acknowledges the linear parametrization of maximal conductances, which are key players in the neuromodulation of neuronal behaviours, from the single-cell to the network scale [7], [9], [29]. At the same time, we highlight the important issue of uncertainty in ion channel models, which define the internal dynamics of a neuron and its synapses. Our first contribution is the design and robustness analysis of a globally convergent adaptive observer based on the classical recursive least-squares (RLS) method, which assumes a linear-in-the-parameter neuronal output dynamics and a known nonlinear internal dynamics. Building on that design, we then propose an augmented adaptive observer capable of estimating parametric (structured) uncertainty in a nonlinearly parameterized neuronal internal dynamics.

The observers in this paper are aligned with the literature on nonlinear adaptive observers [12], [13], [30]. Our approach is however closer to linear observer design [51] than to nonlinear observer design, since, instead of relying on particular state space observer normal forms [2], [22], we rather rely on contraction theory principles [25]. Contraction analysis provides a framework reminiscent of the linear theory of adaptive control, as well as explicit convergence rates and robustness guarantees grounded in the concept of a *virtual system* [3], [49]. Contraction analysis has been a driving methodology in recent adaptive control research [26], [46], and the present work demonstrates its value for the design of adaptive systems

Submitted to IEEE Transactions on Automatic Control. The research leading to these results has received funding from the European Research Council under the Advanced ERC Grant Agreement Switchlet n.670645.

Thiago B. Burghi and Rodolphe Sepulchre are with the Department of Engineering, Control Group, University of Cambridge, CB2 1PZ, UK (e-mails: tbb29@cam.ac.uk, r.sepulchre@eng.cam.ac.uk)

in neuroscience.

The paper is organized as follows. The model structure assumptions and their application to conductance-based models are presented in Section II. In Section III, the online estimation problem for a simplified linear-in-the-parameters model structure is studied, and a globally convergent adaptive observer is presented. In Section IV, parametric nonlinear uncertainty in the internal dynamics is introduced, and we present an augmented adaptive observer to solve the estimation problem; we also discuss the robustness of our designs with respect to unstructured uncertainty, which encompasses model mismatch, time-varying parameters, and measurement errors. In Section V, we illustrate the performance of the adaptive observers and discuss the potential of the approach in neurophysiology.

A. Notation

For a finite-dimensional vector x , we write $n_x := \dim(x)$. For two column vectors x and y , we write $\text{col}(x, y) := (x^\top, y^\top)^\top$. For a matrix $A \in \mathbb{R}^{n \times m}$, $\|A\|$ denotes the spectral norm (the largest singular value of A). For a vector $x \in \mathbb{R}^{n_x}$ and a symmetric matrix $P \in \mathbb{R}^{n_x \times n_x}$, we write $\|x\|_P^2 := x^\top P x$, and $\|x\| := \|x\|_I$ with I the identity matrix. For a vector-valued function $f : \mathbb{R}^{n_1} \times \mathbb{R}^{n_2} \rightarrow \mathbb{R}^m$, we write $\partial_x f(x, y) \in \mathbb{R}^{m \times n_1}$ for the Jacobian of $f(x, y)$ with respect to x . We write $A \succeq B$ ($A \succ B$) if $A - B$ is a positive-semidefinite (positive-definite) matrix. This paper often uses the formalism of contraction analysis [25], which is briefly recalled in Appendix A.

II. SYSTEM CLASS

This section introduces and motivates the model assumptions of the paper. Section II-A defines the basic model structure and states our main assumptions. Section II-B then shows how the model structure and the assumptions are motivated by our main application: the conductance-based model of a neuron. Finally, Section II-C shows that the assumptions extend from single neurons to models of neuronal networks.

A. Problem statement

This paper considers nonlinear state-space systems of the form

$$\dot{v} = \Phi(v, w, u)\theta + a(v, w, u) \quad (1a)$$

$$\dot{w} = A(v, \eta)w + b(v, \eta) \quad (1b)$$

where $v(t) \in \mathbb{R}^{n_v}$ is a measured output, $w(t) \in \mathbb{R}^{n_w}$ are unmeasured internal states, and $\theta \in \mathbb{R}^{n_\theta}$ and $\eta \in \mathbb{R}^{n_\eta}$ are parameter vectors. We call (1a) the *output dynamics*, and (1b) the *internal dynamics*. We assume that Φ , A , a and b are continuously differentiable functions of the appropriate dimensions.

The model structure (1) is motivated by neuroscience applications discussed in Section II-B. In those applications, the vector θ is unknown, while η is not unknown but uncertain. Thus we work in the context of structured model uncertainty [40]. Our aim is to design an adaptive observer to estimate θ

and, if necessary, η . For that purpose, we regard the parameters as part of the state of the system. We will initially consider the constant model

$$\dot{\theta} = 0, \quad \dot{\eta} = 0, \quad (1c)$$

so that $\theta(t) = \theta(0)$ and $\eta(t) = \eta(0)$ for all $t \geq 0$; later, we will study the case where such parameters are time-varying.

We now consider the main assumptions on the properties of (1). These assumptions will also be justified by the applications in Section II-B.

Assumption 1. There exists a compact set U such that $u(t) \in U$ for all $t \geq 0$. Furthermore, there exists a compact convex set $V \times W \times \{\theta(0)\} \times \{\eta(0)\}$ which is positively invariant with respect to (1), uniformly in u on U .

Assumption 2. There exist a symmetric positive definite matrix $M_w \succ 0$ and a contraction rate $\lambda_w > 0$ such that

$$A(v, \eta)^\top M_w + M_w A(v, \eta) \preceq -\lambda_w M_w \quad (2)$$

for all $\{v, \eta\} \in \mathbb{R}^{n_v} \times \mathbb{R}^{n_\eta}$.

Remark 1. When Assumption 1 holds, then without loss of generality we can assume that for all $v \in V$ and $u \in U$, the functions $\Phi(v, w, u)$ and $a(v, w, u)$ are globally Lipschitz and bounded in $w \in \mathbb{R}^{n_w}$. This is because we can replace w by $\varsigma_w(w)$ in the arguments of those functions, where $\varsigma_w : \mathbb{R}^{n_w} \rightarrow W$ is a smooth saturation function such that $\varsigma_w(w) = w$ for all $w \in W$. Doing so does not change the dynamics of (1) within the positively invariant set of Assumption 1.

The reader will note that the system (1) is not in the classical *output-feedback canonical form* [22], nor in any of the equivalent adaptive observer forms summarized by [2]. The system also does not fit the model structures addressed in the more recent adaptive observer literature, e.g., [12], [48].

The next section shows the significance of the model structure (1) and the above assumptions in neurophysiology, hence motivating the observer design of the paper.

B. Conductance-based single-neuron model

Since the seminal work of Hodgkin and Huxley [15], the nonlinear electrical circuits known as conductance-based models have become the foundation of biophysical modelling in neurophysiology (a detailed introduction to those models is found for instance in [18], [20]). We now show that any single-neuron conductance-based model can be written in the form (1) in such a way that Assumptions 1 and 2 are satisfied.

A circuit representation of the model is shown in Figure 1: a capacitor of capacitance $c > 0$ in parallel with a *leak current* I_L and a number of *intrinsic ionic currents* I_{ion} . The *input current* $u(t) \in \mathbb{R}$ represents the external current, injected with an intracellular electrode. The capacitor voltage $v(t) \in \mathbb{R}$ modelling the neuronal membrane potential evolves according to Kirchhoff's law,

$$c \dot{v} = -I_L - \sum_{\text{ion} \in \mathcal{I}} I_{\text{ion}} + u, \quad (3)$$

where $\mathcal{I} = \{\text{ion}_1, \text{ion}_2, \dots, \text{ion}_{\text{card}(\mathcal{I})}\}$ is the (finite) index set of intrinsic ionic currents. Each current in the circuit is

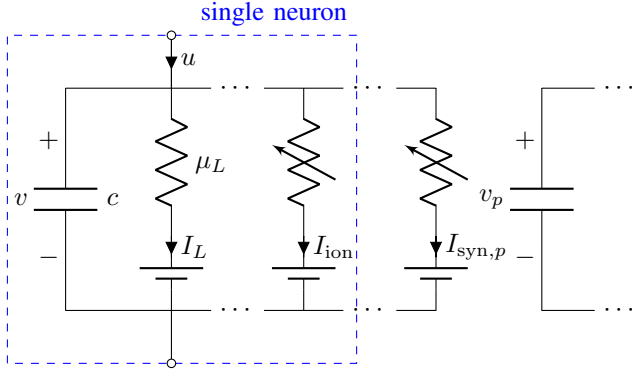


Fig. 1. Circuit representation of a neuron with voltage v that is coupled through a synapse to a presynaptic neuron with voltage v_p .

ohmic in nature, but with a conductance that can be nonlinear and voltage-dependent. The leak current has a constant conductance and is given by

$$I_L = \mu_L(v - \nu_L), \quad (4)$$

with $\mu_L > 0$, and the intrinsic ionic currents are modelled by

$$I_{\text{ion}} = \mu_{\text{ion}} m_{\text{ion}}^{p_{\text{ion}}} h_{\text{ion}}^{q_{\text{ion}}} (v - \nu_{\text{ion}}) \quad (5a)$$

$$\tau_{m_{\text{ion}}}(v) \dot{m}_{\text{ion}} = -m_{\text{ion}} + \sigma_{m_{\text{ion}}}(v) \quad (5b)$$

$$\tau_{h_{\text{ion}}}(v) \dot{h}_{\text{ion}} = -h_{\text{ion}} + \sigma_{h_{\text{ion}}}(v) \quad (5c)$$

The constants $\mu_{\text{ion}} > 0$ and $\nu_{\text{ion}} \in \mathbb{R}$ are called (intrinsic) *maximal conductances* and *reversal potentials*, respectively. The exponents p_{ion} and q_{ion} in (5a) are fixed natural numbers (including zero). The static *activation functions* $\sigma_{m_{\text{ion}}}(v)$ and $\sigma_{h_{\text{ion}}}(v)$, and *time-constant functions* $\tau_{m_{\text{ion}}}(v)$ and $\tau_{h_{\text{ion}}}(v)$, model the nonlinear gating of the ionic conductance. The activation functions are given by sigmoid functions of the form

$$\sigma(v) = \frac{1}{1 + \exp(-(v - \rho)/\kappa)}, \quad (6)$$

where the constants $\rho_{m_{\text{ion}}} \in \mathbb{R}$ and $\rho_{h_{\text{ion}}} \in \mathbb{R}$ determine the *half-activation* of those functions, while the constants $\kappa_{m_{\text{ion}}} > 0$ and $\kappa_{h_{\text{ion}}} < 0$ determine their slopes. Because $\sigma_{m_{\text{ion}}} : \mathbb{R} \rightarrow (0, 1)$ and $\sigma_{h_{\text{ion}}} : \mathbb{R} \rightarrow (0, 1)$ are monotonically increasing and decreasing, respectively, the states m_{ion} and h_{ion} are called *activation* and *inactivation gating variables*, respectively. The time-constant functions are given by bell-shaped functions of the form¹

$$\tau(v) = \underline{\tau} + (\bar{\tau} - \underline{\tau}) \exp(-(v - \zeta)^2/\chi^2) \quad (7)$$

for all $v \in \mathbb{R}$ and some $\underline{\tau}, \bar{\tau} > 0$ and $\zeta, \chi \in \mathbb{R}$.

Example 1. The Hodgkin-Huxley (HH) model [15] includes two intrinsic ionic currents: a transient sodium current I_{Na} and a potassium current I_{K} , so that $\mathcal{I} = \{\text{Na}, \text{K}\}$. The voltage

dynamics of the HH model are given by

$$c \dot{v} = - \underbrace{\mu_{\text{Na}} m_{\text{Na}}^3 h_{\text{Na}}}_{I_{\text{Na}}} (v - \nu_{\text{Na}}) - \underbrace{\mu_{\text{K}} m_{\text{K}}^4}_{I_{\text{K}}} (v - \nu_{\text{K}}) - \underbrace{\mu_{\text{L}}}_{I_{\text{L}}} (v - \nu_{\text{L}}) + u,$$

the dynamics of m_{Na} and m_{K} are given by (5b), and the dynamics of h_{Na} are given by (5c). \triangle

Two basic properties of a single neuron conductance-based model justify the assumptions of Section II-A. The first property is the existence of a positively invariant set, which is a consequence of the fact that all maximal conductances are positive.

Lemma 1. Consider the neuronal model (3)-(7), and assume $|u| \leq \bar{u}$ for all $t \geq 0$. Let

$$\begin{aligned} \bar{v} &:= \max \left\{ \max_{\text{ion} \in \mathcal{I}} \nu_{\text{ion}}, \bar{u} \mu_{\text{L}}^{-1} + \nu_{\text{L}} \right\} \\ \underline{v} &:= \min \left\{ \min_{\text{ion} \in \mathcal{I}} \nu_{\text{ion}}, -\bar{u} \mu_{\text{L}}^{-1} + \nu_{\text{L}} \right\} \end{aligned} \quad (8)$$

Whenever $v(0) \in [\underline{v}, \bar{v}]$, $m_{\text{ion}}(0) \in [0, 1]$ and $h_{\text{ion}}(0) \in [0, 1]$, it follows that

$$v(t) \in [\underline{v}, \bar{v}], \quad m_{\text{ion}}(t) \in [0, 1], \quad \text{and} \quad h_{\text{ion}}(t) \in [0, 1]$$

for all $\text{ion} \in \mathcal{I}$ and all $t \geq 0$.

Proof. See Appendix B.1. \square

The second basic property of a conductance-based model is the contraction of its internal dynamics.

Lemma 2. For all $\text{ion} \in \mathcal{I}$, the dynamics (5b) are globally exponentially contracting, uniformly in v on \mathbb{R} and in $\{\rho_{m_{\text{ion}}}, \kappa_{m_{\text{ion}}}, \zeta_{m_{\text{ion}}}, \chi_{m_{\text{ion}}}\}$ on \mathbb{R}^4 . Exponential contraction holds for any (scalar) constant contraction metric and a contraction rate given by $\bar{\tau}_{m_{\text{ion}}}^{-1}$. The same holds analogously for the dynamics (5c).

Proof. The Jacobian of the vector field of (5b) is $-\tau_{m_{\text{ion}}}^{-1}(v)$. But from (7), we see that for any $p > 0$, the inequality

$$-\tau_{m_{\text{ion}}}^{-1}(v) p - p \tau_{m_{\text{ion}}}^{-1}(v) < -2 \bar{\tau}_{m_{\text{ion}}}^{-1} p$$

holds for any real v , $\rho_{m_{\text{ion}}}$, $\kappa_{m_{\text{ion}}}$, $\zeta_{m_{\text{ion}}}$, and $\chi_{m_{\text{ion}}}$. \square

Finally, we formalize the connection between the single neuron model above and the model structure (1).

Proposition 1. Consider the neuronal model (3)-(7). Let

$$w := (m_{\text{ion}_1}, h_{\text{ion}_1}, m_{\text{ion}_2}, h_{\text{ion}_2}, \dots)^{\top},$$

and let the parameter vector η be composed of any number of elements from the set

$$\bigcup_{i=1}^{n_w} \{\rho_{w_i}, \kappa_{w_i}, \zeta_{w_i}, \chi_{w_i}\}.$$

Let θ be defined according to one of the following parametrizations:

$$\theta := (\mu_{\text{ion}_1}, \mu_{\text{ion}_2}, \dots)^{\top}, \quad \text{or}$$

$$\theta := c^{-1} (1, \mu_{\text{ion}_1}, \mu_{\text{ion}_2}, \dots)^{\top}, \quad \text{or}$$

$$\theta := c^{-1} (1, \mu_{\text{ion}_1}, \mu_{\text{ion}_2}, \dots, \mu_{\text{ion}_1} \nu_{\text{ion}_1}, \mu_{\text{ion}_2} \nu_{\text{ion}_2}, \dots)^{\top}.$$

¹Some models are defined with different types of sigmoids and bell-shaped functions. The results in this paper can be trivially extended to those cases.

Then the neuronal model is of the form (1), and it satisfies Assumptions 1 and 2.

Proof. Given the above parametrization, it can be verified by inspection that (3)-(7) can be written as (1). It then follows immediately from Lemmas 1 and 2 that the neuronal model satisfies Assumptions 1 and 2. \square

As Proposition 1 points out, a conductance-based model can be parametrized in a number of ways. The choice of parametrization depends on implicit assumptions about which model constants are known, and which need to be estimated. Estimation of the maximal conductances μ_{ion} is of particular importance in neurophysiological applications, as they can be regarded as the key parameters for *adaptive* control of a neuronal network [7]–[9]. Maximal conductances model the levels of expression of particular types of ion channels in the neuronal membrane [14], and these levels vary greatly under the biochemical action of neuromodulators [29]. In contrast, many other constants in a neuron model may be assumed to be known, but with some level of uncertainty.

Example 2. Assume that the capacitance, maximal conductances and half-activations of the HH model of Example 1 need to be estimated, while other model constants are known. Then we may define $w := (m_{\text{Na}}, h_{\text{Na}}, m_{\text{K}})^{\top}$ and

$$\begin{aligned}\theta &:= c^{-1} (1, \mu_{\text{Na}}, \mu_{\text{K}}, \mu_{\text{L}})^{\top} \\ \eta &:= (\rho_{m_{\text{Na}}}, \rho_{h_{\text{Na}}}, \rho_{m_{\text{K}}})^{\top}\end{aligned}$$

so that the dynamics of the HH model are given by (1), with

$$\begin{aligned}\Phi(v, w, u) &= -(-u, w_1^3 w_2 (v - \nu_{\text{Na}}), w_3^4 (v - \nu_{\text{K}}), (v - \nu_{\text{L}})) \\ A(v) &= -\text{diag}(\tau_{m_{\text{Na}}}^{-1}(v), \tau_{h_{\text{Na}}}^{-1}(v), \tau_{m_{\text{K}}}^{-1}(v)) \\ b(v, \eta) &= -A(v) \text{diag}(\sigma_{m_{\text{Na}}}(v), \sigma_{h_{\text{Na}}}(v), \sigma_{m_{\text{K}}}(v))\end{aligned}$$

and $a = 0$. \triangle

C. Conductance-based neural network model

The two basic properties of single neuron models discussed in the previous section extend to conductance-based network models. A conductance-based neural network is given by the interconnection of $n_v \in \mathbb{N}$ single neurons via *synapses*. For $i \in \mathcal{N} := \{1, \dots, n_v\}$, the voltage dynamics of the i^{th} neuron in the network is described by

$$c \dot{v}_i = -I_{\text{L},i} - \sum_{\text{ion} \in \mathcal{I}} I_{\text{ion},i} - \sum_{\text{syn} \in \mathcal{S}} \sum_{p \in \mathcal{P}} I_{\text{syn},p,i} + u_i \quad (9)$$

where each $I_{\text{L},i}$ is given by (4) and each $I_{\text{ion},i}$ is given by (5), as before (in this case a subscript i is attached to all variables). The additional currents $I_{\text{syn},p,i}$ above are *synaptic currents* interconnecting the i^{th} (postsynaptic) neuron with the p^{th} (presynaptic) neuron, so that $\mathcal{P} \subseteq \mathcal{N}$. Since there might exist multiple synapses (based on different neurotransmitters) connecting two neurons, we denote each synaptic type by syn , and the index set of synaptic types by \mathcal{S} .

Synaptic currents arise from electrochemical connections between neurons [11, Chapter 7]. We consider the model used

in [6], [11], which can be written as

$$I_{\text{syn},p} = \mu_{\text{syn},p} s_{\text{syn},p} (v - \nu_{\text{syn}}) \quad (10a)$$

$$\tau_{\text{syn}}(v_p) \dot{s}_{\text{syn},p} = -s_{\text{syn},p} + a_{\text{syn}} \tau_{\text{syn}}(v_p) \sigma_{\text{syn}}(v_p) \quad (10b)$$

with a synaptic time-constant function τ_{syn} given by

$$\tau_{\text{syn}}(v_p) = \frac{1}{a_{\text{syn}} \sigma_{\text{syn}}(v_p) + b_{\text{syn}}} \quad (11)$$

and a synaptic activation function σ_{syn} of the form (6), with $\rho_{\text{syn}} \in \mathbb{R}$ and $\kappa_{\text{syn}} > 0$. Here, $s_{\text{syn},p}$ is the synaptic gating variable, v_p is the membrane voltage of the presynaptic neuron, and $a_{\text{syn}} > 0$ and $b_{\text{syn}} > 0$ are constant parameters. The constants $\mu_{\text{syn},p} > 0$ and $\nu_{\text{syn}} \in \mathbb{R}$ are (synaptic) maximal conductances and reversal potentials, respectively. Notice that $0 < (a_{\text{syn}} + b_{\text{syn}})^{-1} \leq \tau_{\text{syn}}(v_p) \leq b_{\text{syn}}^{-1}$ for all $v_p \in \mathbb{R}$.

Proposition 2. Consider a conductance-based neural network model with voltage output vector $v = (v_1, \dots, v_{n_v})^{\top}$ and internal state vector $w := \text{col}(w^{(1)}, \dots, w^{(n_v)})$ where

$$w^{(i)} := (m_{\text{ion}_1,i}, \dots, s_{\text{syn}_1,1,i}, s_{\text{syn}_2,1,i}, \dots, s_{\text{syn}_1,2,i}, \dots)$$

collects the intrinsic and synaptic gating variables of the i^{th} neuron. Let each neuron in the network be parametrized as in Proposition 1, allowing for the inclusion of μ_{syn} and ν_{syn} in θ , and for the inclusion of ρ_{syn} , κ_{syn} , ζ_{syn} and χ_{syn} in η . Then the network model is of the form (1), and it satisfies Assumptions 1 and 2.

Since Proposition 2 is a trivial extension of Proposition 1, we omit its proof and present a concrete example instead:

Example 3. A Half-Center Oscillator (HCO) is a circuit composed of two neurons mutually coupled by inhibitory synapses. This elementary network is the simplest example of a Central Pattern Generator, a type of neural network that plays an important role in the generation of autonomous rhythms for motor control [28]. A simple HCO model is obtained by interconnecting two HH neurons with a GABA-type² synaptic current I_{G} , and adding to each of the neurons an intrinsic calcium current I_{Ca} [6]. This results in $\mathcal{I} = \{\text{Na}, \text{K}, \text{Ca}\}$, $\mathcal{S} = \{\text{G}\}$, and voltage dynamics given by

$$\begin{aligned}c_i \dot{v}_i &= -\mu_{\text{Na},i} m_{\text{Na},i}^3 h_{\text{Na},i} (v_i - \nu_{\text{Na}}) - \mu_{\text{K},i} m_{\text{K},i}^4 (v_i - \nu_{\text{K}}) \\ &\quad - \mu_{\text{Ca},i} m_{\text{Ca},i}^3 h_{\text{Ca},i} (v_i - \nu_{\text{Ca}}) - \mu_{\text{G},p,i} s_{\text{G},p,i} (v_i - \nu_{\text{G}}) \\ &\quad - \mu_{\text{L},i} (v_i - \nu_{\text{L}}) + u_i\end{aligned}$$

for $i, p \in \mathcal{N} = \{1, 2\}$ and $p \neq i$. The gating variables of each neuron, which evolve according to (5b)-(5b) and (10b), are collected in $w^{(i)} = (m_{\text{Na},i}, h_{\text{Na},i}, m_{\text{K},i}, m_{\text{Ca},i}, h_{\text{Ca},i}, s_{\text{G},i,p})^{\top}$. Now let

$$\mu^{(i)} = (\mu_{\text{Na},i}, \mu_{\text{K},i}, \mu_{\text{Ca},i}, \mu_{\text{G},p,i}, \mu_{\text{L},i})^{\top} \quad (12)$$

for $i, p \in \mathcal{N} = \{1, 2\}$ and $p \neq i$. Then we can parameterize the HCO according to

$$\theta = \text{col}(\mu^{(1)}, \mu^{(2)}) \quad (13)$$

²Gamma-aminobutyric acid (GABA) is a neurotransmitter associated with inhibitory synapses.

with $\mu^{(1)}$ and $\mu^{(2)}$ given by (12). Letting $v = (v_1, v_2)^\top$ and $w = \text{col}(w^{(1)}, w^{(2)})$, the voltage dynamics of the model can then be written as (1a), where

$$\Phi(v, w) = \begin{bmatrix} \varphi(v_1, w^{(1)}) & 0 \\ 0 & \varphi(v_2, w^{(2)}) \end{bmatrix}$$

$$a(t) = (u_1(t)/c_1, u_2(t)/c_2)^\top$$

with

$$\varphi(v_i, w^{(i)}) = -\frac{1}{c_i} \begin{pmatrix} m_{\text{Na},i}^3 h_{\text{Na},i} (v_i - \nu_{\text{Na}}) \\ m_{\text{K},i}^4 (v_i - \nu_{\text{K}}) \\ m_{\text{Ca},i}^3 h_{\text{Ca},i} (v_i - \nu_{\text{Ca}}) \\ s_{\text{G},p,i} (v_i - \nu_{\text{G}}) \\ v_i - \nu_{\text{L}} \end{pmatrix}^\top$$

for $i = 1, 2$ and $p \neq i$. \triangle

III. ESTIMATION OF THE OUTPUT DYNAMICS

In this section, we simplify the problem statement of Section II-A by considering the case in which there is no uncertain parameter η , that is, the internal dynamics are assumed to be perfectly known. Hence we consider the simplified model structure

$$\dot{v} = \Phi(v, w, u)\theta + a(v, w, u) \quad (14a)$$

$$\dot{w} = A(v)w + b(v) \quad (14b)$$

$$\dot{\theta} = 0 \quad (14c)$$

satisfying Assumptions 1 and 2. This simplified model already deserves attention. In Section III-A, we illustrate how a naive output-error estimation scheme leads to issues. Then, using the basic properties of Section II, we propose a recursive least-squares (RLS) algorithm in Section III-B, and a RLS-based adaptive observer in Section III-C.

A. Challenges in neuronal model estimation

The neuronal behaviours displayed by conductance-based models range from the simple spiking oscillations of single neurons to the large-scale rhythmic computations performed by cortical networks [50]. This is because despite the fact that conductance-based models have contracting internal dynamics, their overall dynamics are in general non-contracting. In the terminology of linear systems, they have stable zeros, but possibly unstable poles. In biophysical terms, this happens due to intrinsic ionic currents with a negative differential conductance, a source of positive feedback and instability [42].

Example 4. Consider the HH model of Example 1, with reversal potentials such that $\nu_{\text{K}} < \nu_{\text{L}} < \nu_{\text{Na}}$. For any input current such that $|u(t)| < \mu_{\text{L}}(\nu_{\text{Na}} - \nu_{\text{L}})$ for all $t \geq 0$, the voltage bounds from Lemma 1 show that the membrane voltage satisfies $v < \nu_{\text{Na}}$ for all $t \geq 0$. This implies that

$$-\partial_{m_{\text{Na}}} I_{\text{Na}} \partial_v \dot{m}_{\text{Na}} > 0$$

at any admissible equilibrium of the system, and thus the Sodium current I_{Na} introduces positive feedback to the membrane voltage of the HH model. \triangle

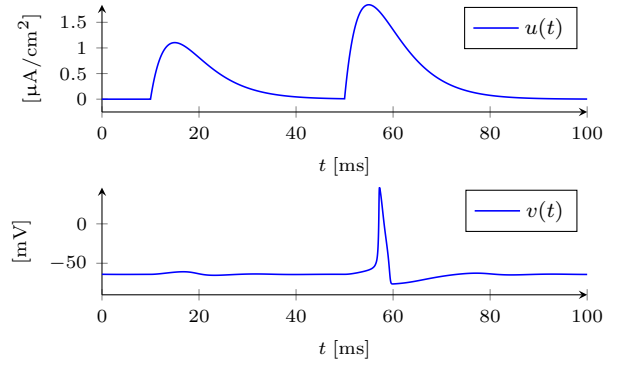


Fig. 2. Excitability in the HH model. A small current pulse causes no spike, while a larger current pulse causes a spike. HH parameter values are described in Table I and Appendix C.1.

The non-contracting nature of neuronal dynamics is the main reason why traditional parameter estimation methods based on *output-error* (or *simulation-error*) criteria [24], [27] cannot be effectively applied to conductance-based models. This is illustrated by means of a numerical example:

Example 5. Consider the typical biophysical parameters of the HH model shown in Table I below. Owing to the large value of μ_{Na} , the positive feedback introduced by the Sodium current I_{Na} dominates the model dynamics in some regions of the state-space [18]. Using these parameters, Figure 2 illustrates the excitability of the model.

Now, consider the parametrization given by $\theta = \mu_{\text{Na}}$, and suppose μ_{Na} must be estimated from the continuous-time measurements $u(t)$ and $v(t)$ shown in Figure 2. In a naive application of the prediction-error method [24], a *predictor model* would be given by

$$\begin{aligned} \dot{v} &= -\hat{\mu}_{\text{Na}} \hat{m}_{\text{Na}}^3 \hat{h}_{\text{Na}} (\hat{v} - \nu_{\text{Na}}) + a(\hat{v}, \hat{m}_{\text{K}}, u) \\ \dot{\hat{w}} &= A(\hat{v})\hat{w} + b(\hat{v}) \end{aligned} \quad (15)$$

with $\hat{w} = (\hat{m}_{\text{Na}}, \hat{h}_{\text{Na}}, \hat{m}_{\text{K}})^\top$ and

$$a(\hat{v}, \hat{m}_{\text{K}}, u) = -\mu_{\text{K}} \hat{m}_{\text{K}}^4 (\hat{v} - \nu_{\text{K}}) - \mu_{\text{L}} (\hat{v} - \nu_{\text{L}}) + u$$

The estimate $\hat{\mu}_{\text{Na}}$ is then obtained by minimizing the *output-error* cost function

$$V(\hat{\mu}_{\text{Na}}, \hat{w}(0), T) = \frac{1}{T} \int_0^T (v(t) - \hat{v}(t))^2 dt \quad (16)$$

in $\hat{\mu}_{\text{Na}}$ and $\hat{w}(0)$. The issue with this approach is that it may not be trivial to find a global minimum for $\hat{\mu}_{\text{Na}}$ using numerical methods, even when the problem is simplified by fixing $(\hat{v}(0), \hat{w}(0)) = (v(0), w(0))$. The reason can be visualized in Figure 3, where we have plotted the cost function $V(\hat{\mu}_{\text{Na}}, w(0), T)$ obtained with the input-output traces from Figure 2 ($T = 100$). It can be seen that the cost function

TABLE I
PARAMETERS OF THE HH MODEL [16], [18].

μ_{Na}	μ_{K}	μ_{L}	ν_{Na}	ν_{K}	ν_{L}	c
120	36	0.3	55	-77	-54.4	1

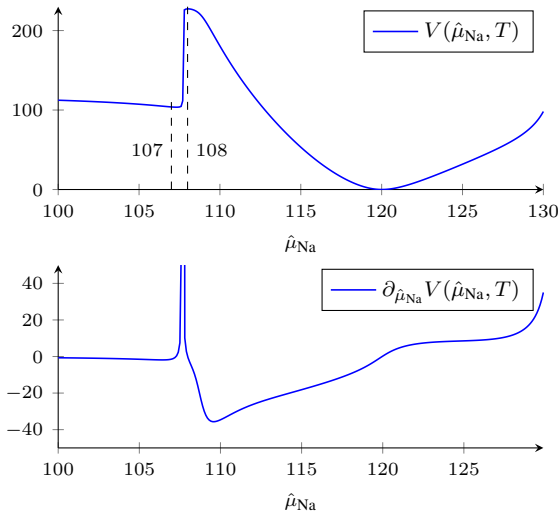


Fig. 3. Cost function $V(\hat{\mu}_{\text{Na}}, w(0), T)$ given by (16) and its gradient.

is nearly discontinuous between $\hat{\mu}_{\text{Na}} = 107$ and $\hat{\mu}_{\text{Na}} = 108$. The behaviour underlying this near discontinuity is unveiled in Figure 4, where two solutions of (15) are plotted corresponding to the estimates $\hat{\mu}_{\text{Na}} = 107$ and $\hat{\mu}_{\text{Na}} = 108$. It is the spike which appears when increasing $\hat{\mu}_{\text{Na}}$ that causes a sudden change in the cost function. The cost function contains one near discontinuity, since there is a single spike being fired. For a dataset with multiple spikes, the cost function would rapidly become intractable.

△

Example 5 illustrates the more general problem of lack of tractability in estimating the parameters of a non-contracting system with an output-error criterion [1], [39]. In fact, the lack of contraction is the root cause of what has been called the “exploding gradient” problem in deep learning theory [37]. The exploding gradient is clearly visible in Figure 3.

B. Least Squares and reduced-order observer

To remedy the instability illustrated in Example 5, we can make use of the following remark:

Remark 2. Assumption 2 implies that the system

$$\dot{\hat{w}} = A(v)\hat{w} + b(v) \quad (17)$$

is a globally exponentially convergent reduced-order identity observer for the dynamics (14b). More precisely, as $t \rightarrow \infty$ we have $\hat{w}(t) \rightarrow w(t)$ for any piecewise continuous $v(t)$ and any initial conditions $\hat{w}(0), w(0) \in \mathbb{R}^{n_w}$.

We employ the reduced-order observer (17) to obtain estimates \hat{w} of the internal states w . Contraction of the internal states suggests postulating the predictor model

$$\dot{\hat{v}} = \Phi(v, \hat{w}, u)\hat{\theta} + a(v, \hat{w}, u) \quad (18a)$$

$$\dot{\hat{w}} = A(v)\hat{w} + b(v) \quad (18b)$$

which, in the particular case of Example 5, amounts to replacing \hat{v} by v in the right-hand side of (15).

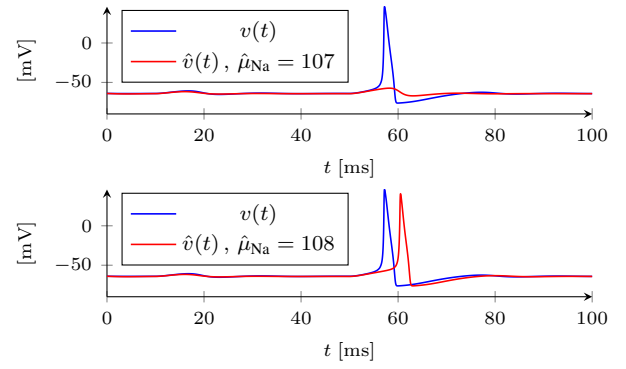


Fig. 4. Solutions of the HH predictor (15) for two values of $\hat{\mu}_{\text{Na}}$ (red), compared to the solution of the true model displayed in Figure 2 (blue).

Notice that, for $\hat{w} = w$, the voltage predictor model (18a) acquires a continuous-time *equation-error* model structure [24], [45]. Classical system identification theory [45, Section 2] thus suggests performing parameter estimation by solving the regularized problem

$$\hat{\theta}(T) = \min_{\hat{\theta}} V(\hat{\theta}, T) + \hat{\theta}^T R_0(T) \theta \quad (19)$$

with the weighted cost function

$$V(\hat{\theta}, T) = \frac{1}{T} \int_0^T e^{-\alpha(T-\tau)} \|H\dot{v}(\tau) - H\hat{v}(\tau)\|^2 d\tau \quad (20)$$

where $\alpha > 0$ is a *forgetting factor*, introduced to discount the initial error between $w(0)$ and $\hat{w}(0)$, R_0 is a symmetric positive semidefinite matrix, and H is the operator of a strictly proper LTI filter introduced to avoid differentiating $v(t)$. Choosing the simple filter

$$H(s) = \frac{\gamma}{s + \gamma} \quad (21)$$

leads to

$$\begin{aligned} H\dot{\hat{v}}(t) &= \gamma\Psi(t)\hat{\theta} + H\hat{a}(t) \\ \dot{\Psi}(t) &= -\gamma\Psi(t) + \Phi(v(t), \hat{w}(t), u(t)) \\ \hat{a}(t) &= a(v(t), \hat{w}(t), u(t)) \end{aligned} \quad (22)$$

which shows that (19)-(20) is now quadratic in $\hat{\theta}$ (notice $H\dot{v}$ is obtained by filtering the data v with $sH(s)$). It follows that the batch-mode problem (19) admits a well-known solution based on the normal equation [45, p. 55]. That $\hat{\theta}(T) \rightarrow \theta$ as $T \rightarrow \infty$ will be shown to be a consequence of the convergence properties of the adaptive observer introduced in Section III-C.

C. RLS-based adaptive observer

Consider the system (14). An adaptive observer for this system is given by

$$\begin{aligned} \dot{\hat{v}} &= \Phi(v, \hat{w}, u)\hat{\theta} + a(v, \hat{w}, u) + \gamma(I + \Psi P \Psi^T)(v - \hat{v}) \\ \dot{\hat{w}} &= A(v)\hat{w} + b(v) \\ \dot{\hat{\theta}} &= \gamma P \Psi^T (v - \hat{v}) \end{aligned} \quad (23)$$

where $\gamma > 0$ is a constant gain, and the matrices P and Ψ evolve according to

$$\dot{\Psi} = -\gamma\Psi + \Phi(v, \hat{w}, u), \quad \Psi(0) = 0 \quad (24a)$$

$$\dot{P} = \alpha P - \gamma P \Psi^\top \Psi P, \quad P(0) \succ 0 \quad (24b)$$

where $\alpha > 0$ is a constant forgetting rate. The assumption that $\Psi(0) = 0$ is made without loss of generality.

Remark 3. The adaptive observer (23)-(24) relates to a number of designs in the literature. For instance, when we remove the internal dynamics ($n_w = 0$) and set $\alpha = \gamma$, then (23)-(24) is similar to the high-gain design proposed in [12]. Also, if $w(t)$ is assumed to be known, then by replacing \hat{w} by w in (23) we recover a nonlinear variant of the classical linear design of [51]. Finally, setting $P = I$ and $\Psi = \Phi$, and removing the adaptive gain and its dynamics (24), it reduces to the design proposed in [2], which can be thought of as being based on the Least-mean squares algorithm rather than RLS.

We will show that the convergence of the adaptive observer above does not require a high gain; a discussion on the benefits of tuning α and γ will also be presented in Section IV-C. Furthermore, we can prove the design (23)-(24) is directly connected to the least-squares problem discussed earlier:

Proposition 3. *The adaptive observer (23)-(24) implements the recursive least squares (RLS) solution of the least squares problem given by (19)-(22), with $R_0(T) = e^{-\alpha T} P^{-1}(0)/T$.*

Proof. See Appendix B.2. \square

To show exponential convergence of the adaptive observer, we require a standard persistent excitation condition (see, for instance, [2], [12], [47]):

Definition 1. A time-varying matrix $M(t)$ is said to be persistently exciting (PE) if there exist $T > 0$ and $\delta > 0$ such that for all $t \geq 0$, we have

$$\int_t^{t+T} M(\tau)M(\tau)^\top d\tau \succeq \delta I$$

Assumption 3. The signals $v(t)$ and $u(t)$ are such that for any trajectory of (23), the matrix $\Psi(t)^\top$ is persistently exciting.

It is well-known [51] that Assumption 3 ensures uniform positive-definiteness of $P(t)$. In our context, we have:

Lemma 3. *Under Assumptions 1 to 3 there exist positive constants $\underline{p} > 0$ and*

$$\bar{p} = \min \{ e^{-\alpha T} \lambda_{\min}[R(0)], \delta \gamma e^{-2\alpha T} \}^{-1} \quad (25)$$

such that

$$\underline{p} \leq P(t) \leq \bar{p} \quad (26)$$

for all $t \geq 0$.

Proof. See Appendix B.3. \square

We can now state a global convergence result³ for the simple adaptive observer (23)-(24).

³Theorem 1 can also be proven with classical (non-differential) Lyapunov arguments, in the fashion of [12], [51]. Our proof relies instead on contraction (differential) analysis, which is useful to the results of the next section.

Theorem 1. *Consider the systems (14) and (23)-(24), and let Assumptions 1 to 3 hold. Let $\gamma > 0$ and $\alpha > 0$. Then, globally, we have*

$$\text{col}(\hat{v}(t), \hat{w}(t), \hat{\theta}(t)) \rightarrow \text{col}(v(t), w(t), \theta)$$

exponentially fast as $t \rightarrow \infty$, with a convergence rate given by arbitrary $\lambda < \min\{\alpha, \lambda_w, \gamma\}$.

Proof. See Appendix B.4. \square

One should notice that the persistent excitation Assumption 3 is classical yet difficult to check in practice, since it depends on system trajectories of a nonlinear system. However, the excitable (spiking) behavior of the neuronal circuits considered in this paper is an excellent source of excitation that can be reliably tapped through the application of superthreshold applied currents.

IV. ESTIMATION UNDER UNCERTAINTY

The design in the previous section assumes no uncertainty in the model, which is unrealistic in a biophysical context. This section addresses different forms of uncertainty. Section IV-A deals with *structured uncertainty* in the internal dynamics, modelled by the uncertain parameter η in (1b). Building on the design (23)-(24), we present a locally convergent adaptive observer capable of estimating η in addition to the unknown parameters θ in (1a). Section IV-B then discusses the problem of measurement errors and how the adaptive observer can be modified to mitigate that problem. Finally, Section IV-C discusses the robustness of the adaptive observers with respect to unstructured uncertainty in the form of model mismatch and time-varying parameters.

A. Estimating uncertain internal dynamics parameters

To deal with structured uncertainty in the internal dynamics of (1), we augment the simple adaptive observer (23) to estimate the parameter vector η as well. To design the observer the following is assumed:

Assumption 4. Assume that compact sets $\Theta \in \mathbb{R}^{n_\theta}$ and $H \in \mathbb{R}^{n_\eta}$ are known such that $\theta \in \Theta$ and $\eta \in H$.

Remark 4. Analogously to Remark 1, under Assumptions 1 and 4, we can assume without loss of generality that for all $v \in V$, the functions $A(v, \eta)$ and $b(v, \eta)$ are globally Lipschitz and bounded in $\eta \in \mathbb{R}^{n_\eta}$.

The augmented adaptive observer is given by

$$\begin{aligned} \dot{\hat{v}} &= \Phi(v, \hat{w}, u)\hat{\theta} + a(v, \hat{w}, u) + \gamma(I + \Psi_v P \Psi_v^\top)(v - \hat{v}) \\ \dot{\hat{w}} &= A(v, \hat{\eta})\hat{w} + b(v, \hat{\eta}) + \gamma\Psi_w P \Psi_w^\top(v - \hat{v}) \\ \text{col}(\dot{\hat{\theta}}, \dot{\hat{\eta}}) &= \gamma P \Psi_v^\top(v - \hat{v}) \end{aligned} \quad (27)$$

where $\gamma > 0$ is a constant gain, and the matrices P and

$$\Psi := \text{col}(\Psi_v, \Psi_w)$$

evolve according to

$$\dot{\Psi} = A_\Psi(t)\Psi + B_\Psi(t) \quad (28a)$$

$$\dot{P} = \alpha P + \beta P^2 - \gamma P \Psi_v^\top \Psi_v P \quad (28b)$$

where $\alpha, \beta > 0$ are constant hyperparameters, and the matrix functions in (24a) are given by

$$A_\Psi(t) = \begin{bmatrix} -\gamma I & \partial_{\hat{w}}[\Phi(v, \hat{w}, u)\varsigma_\theta(\hat{\theta}) + a(v, \hat{w}, u)] \\ 0_{n_w \times n_v} & A(v, \hat{\eta}) \end{bmatrix}$$

and

$$B_\Psi(t) = \begin{bmatrix} \Phi(v, \hat{w}, u) & 0_{n_v \times n_\eta} \\ 0_{n_w \times n_{\theta_v}} & \partial_{\hat{\eta}}[A(v, \hat{\eta})\varsigma_w(\hat{w}) + b(v, \hat{\eta})] \end{bmatrix}$$

with ς_θ and ς_η smooth saturation functions (see Remark 1). Here, we assume without loss of generality that $\Psi_v(0) = 0$, $\Psi_w(0) = 0$, and $P(0) \succ 0$.

As before we need a persistent excitation condition:

Assumption 5. The signals $v(t)$ and $u(t)$ are such that for any trajectory of (27), the matrix $\Psi_v(t)^\top$ is persistently exciting.

Notice that for $\alpha > 0$ Assumption 5 implies that the pair $(-\frac{\alpha}{2}I, \Psi_v(t))$ is uniformly observable in the sense of [38]. In this case, for $\beta > 0$ the main result of [38] shows that $P(t)$ satisfies (26) for some $\bar{p}, \underline{p} > 0$ for all $t \geq 0$. If $\beta = 0$, Lemma 3 still applies. Letting

$$x(t) = \text{col}(v(t), w(t), \theta(t), \eta(t))$$

and analogously for $\hat{x}(t)$, we have the following result:

Theorem 2. Let Assumptions 1, 2, 4 and 5 hold. Then for any $\alpha, \gamma > 0$, $\beta \geq 0$, and $\lambda < \min\{\alpha, \lambda_w, \gamma\}$, for $\hat{x}(0)$ sufficiently close to $x(t)$, we have $\hat{x}(t) \rightarrow x(t)$ as $t \rightarrow \infty$, exponentially fast, with rate λ .

Proof. See Appendix B.5. \square

Remark 5. The observer above is a natural extension of the simpler observer (23)-(24). Indeed, if A and b are independent of η , then we recover (23)-(24) from (27)-(28): in this case, $\partial_{\hat{\eta}}[A(v)\varsigma_w(\hat{w}) + b(v)] = 0$, and $\dot{\Psi}_w = A(v)\Psi_w$ in (24a). Thus, if $\Psi_w(0) = 0$ we have $\Psi_w(t) = 0$ for all $t \geq 0$ and (23)-(24) is recovered. If $\Psi_w(0) \neq 0$, then $\Psi_w \rightarrow 0$ as $t \rightarrow \infty$ by Assumption 2, and the simpler observer is also recovered.

Remark 6. Writing $\Psi_w = [\Psi_{w,1} \ \Psi_{w,2}]$ with $\Psi_{w,1} \in \mathbb{R}^{n_w \times n_{\theta_v}}$ and $\Psi_{w,2} \in \mathbb{R}^{n_w \times n_\eta}$, by Assumption 2 we have without loss of generality that $\Psi_{w,1} = 0$. Furthermore, Assumption 5 is in a sense also a condition on the excitation of $\Psi_{w,2}$. To see this, write $\Psi_v = [\Psi_{v,1} \ \Psi_{v,2}]$ analogously. Then from (28a) the dynamics of $\Psi_{v,1}$ are solely driven by $\Phi(v, \hat{w}, u)$, while the dynamics of $\Psi_{v,2}$ are solely driven by $\partial_{\hat{w}}[\Phi(v, \hat{w}, u)\varsigma_\theta(\hat{\theta}) + a(v, \hat{w}, u)]\Psi_{v,2}$. Thus part of the persistent excitation of Ψ_v is directly due to $\Psi_{w,2}$.

B. Measurement errors

The adaptive observer design of Section IV-A relies on *output injection*, that is, it assumes that the measurement $y = v$ has no errors, and injects the measured v in the observer dynamics. This corresponds to an *equation error* model structure [24]. Assume instead that a measurement error $e(t)$ is present, so that

$$y(t) = v(t) + e(t) \quad (30)$$

In this case, (27)-(28) must be redefined by replacing $v(t)$ with $y(t)$. It is clear that this introduces measurement errors in the observer dynamics, and it is well known that even if some level of stability is retained, the parameter estimates will be biased. If the bias is too large, one could modify (27)-(28) towards an *output error* model structure by replacing $v(t)$ with $\hat{v}(t)$ in the arguments of Φ , A , a , and b . The downside of the output-error approach (discussed in a *batch* context in Section III-A) is that convergence of the adaptive observer may be lost even when the measurements have no errors (the *nominal* case $y = v$). More precisely, a convergence analysis analogous to that of Theorem 2 shows that nominal stability of the output error-based adaptive observer only holds for sufficiently high values of γ . But a high γ is undesirable when measurement errors do occur, as γ contributes to perturbations in the dynamics such as $\gamma(I + \Psi_y P \Psi_y^\top)e$ and $\gamma \Psi_w P \Psi_y^\top e$.

To leverage the advantages of both equation error and output error approaches (lower gain γ and lower bias, respectively), we can exploit an additional property of the true system, motivated by the neuronal systems of Section II-B:

Assumption 6. Under Assumption 1, there exist a symmetric positive definite matrix $M_v \succ 0$ and a contraction rate $\lambda_v > 0$ such that

$$\partial_v[\Phi\theta + a]^\top M_v + M_v \partial_v[\Phi\theta + a] \preceq -\lambda_v M_v$$

for all $\{v, w, \theta\} \in V \times W \times \{\theta(0)\}$.

Remark 7. For any conductance-based model from Section II-B, Assumption 6 holds with $M_v = I$ and $\lambda_v = -2\mu_L/c$.

Assumption 6 motivates the observer structure given by

$$\begin{aligned} \dot{\hat{v}} &= \Phi(\hat{v}, \hat{w}, u)\hat{\theta} + a(\hat{v}, \hat{w}, u) + \gamma(I + \Psi_v P \Psi_v^\top)(y - \hat{v}) \\ \dot{\hat{w}} &= A(y, \hat{\eta})\hat{w} + b(y, \hat{\eta}) + \gamma \Psi_w P \Psi_v^\top (y - \hat{v}) \end{aligned}$$

$$\text{col}(\dot{\hat{\theta}}, \dot{\hat{\eta}}) = \gamma P \Psi_v^\top (y - \hat{v})$$

and by (28), where A_Ψ and B_Ψ are replaced by

$$A_\Psi(t) = \begin{bmatrix} -\gamma I + \partial_{\hat{v}}[\hat{\Phi}\varsigma_\theta(\hat{\theta}) + \hat{a}] & \partial_{\hat{w}}[\hat{\Phi}\varsigma_\theta(\hat{\theta}) + \hat{a}] \\ 0_{n_w \times n_v} & A(\hat{v}, \hat{\eta}) \end{bmatrix}$$

and

$$B_\Psi(t) = \begin{bmatrix} \hat{\Phi} & 0_{n_v \times n_\eta} \\ 0_{n_w \times n_{\theta_v}} & \partial_{\hat{\eta}}[A(y, \hat{\eta})\varsigma_w(\hat{w}) + b(y, \hat{\eta})] \end{bmatrix}$$

where $\hat{\Phi} = \Phi(\hat{v}, \hat{w}, u)$ and $\hat{a} = a(\hat{v}, \hat{w}, u)$. The following nominal convergence result is immediate:

Theorem 3. Under Assumption 6, for $y = v$, the statement of Theorem 2 also applies to the adaptive observer above.

Proof. The proof follows the very same steps as that of Theorem 2, and is hence omitted. \square

1) **Robustness:** The contraction results of Theorems 1 to 3 imply a nominal exponential stability property of the adaptive observer trajectories. Given those results, it is not difficult to show that the convergence properties of the adaptive observers presented above all have some level of robustness with respect to measurement errors of the form (30). A contraction-based robustness analysis along the lines of [3, Section III]

can be performed to show that for a bounded error $e(t)$ and sufficiently small $\sup_{t \geq 0} \|e(t)\|$, the trajectories of the adaptive observer estimates remain close to the trajectories of the true system states. Since this analysis is also similar to the robustness result presented in the next section, we will omit it here, and rather evaluate the robustness to measurement noise by means of simulations in Section V-A.

C. Robustness to unstructured uncertainty

It is well known that with exponential contraction comes robustness with respect to sufficiently small perturbations [25]. In this section, we discuss how this robustness manifests in the context of the observers studied in this paper. To keep the discussion conceptual, we consider the perturbed model

$$\dot{v} = \Phi(v, w, u)\theta + a(v, w, u) + d_v(t, v, w, \theta) \quad (32a)$$

$$\dot{w} = A(v)w + b(v) + d_w(t, v, w) \quad (32b)$$

$$\dot{\theta} = d_\theta(t, v, w) \quad (32c)$$

where $d := \text{col}(d_v, d_w, d_\theta)$ models an unstructured uncertainty. The disturbances d_v and d_w can be interpreted as *model mismatch* resulting from unmodelled dynamics, while d_θ models the variation over time of the unknown parameters.

We will show that the adaptive observer (23)-(24) yields online estimates $\hat{\theta}(t)$ that track the time-varying $\theta(t)$ in an approximate sense; we also remark that the analysis presented in this section can be extended to the augmented observers of Sections IV-A and IV-B, in which case the result becomes local. We require the following boundedness assumption:

Assumption 7. The solution $\text{col}(v, w, \theta)$ of (32) remains in the compact set $V \times W \times \Theta$ for all $t \geq 0$. Furthermore, for some $\bar{d}_v > 0$, we have $\|d_v(t, x)\| \leq \bar{d}_v$ for all $t \geq 0$, and analogously for d_w and d_θ .

Proposition 4. Let Assumptions 1 to 3 and 7 hold, and consider any solutions $x(t) = \text{col}(v(t), w(t), \theta(t))$ of the true system (32) and $\hat{x}(t) = \text{col}(\hat{v}(t), \hat{w}(t), \hat{\theta}(t))$ of the observer (23)-(24) such that $x(0) \in V \times W \times \Theta$ and $\hat{x} \in \mathbb{R}^{n_v+n_w+n_{\theta_v}}$. Let $\alpha, \gamma > 0$ and $\lambda < \min\{\alpha, \lambda_w, \gamma\}$. Then $\hat{x}(t)$ converges exponentially fast, with rate λ , towards the ball

$$\mathcal{B}_{r,D}(x(t)) := \{\hat{x} : \|\hat{x} - x(t)\|_D^2 \leq r^2\}$$

centred at $x(t)$, with respect to the metric

$$D = \text{diag} \left(\frac{\varepsilon \bar{p}^{-1}}{1 + \bar{p}^{-1} + \bar{\Psi}^2} I, \lambda_{\min}[M_w] I, \frac{\varepsilon \bar{p}^{-1}}{1 + \bar{\Psi}^2} I \right), \quad (33)$$

and of constant radius r given by

$$r^2 = \frac{\varepsilon \bar{d}_v^2 + \lambda_{\max}[M_w] \bar{d}_w^2 + \varepsilon (\bar{\Psi}^2 + \underline{p}^{-1}) \bar{d}_\theta^2}{\lambda^2} \quad (34)$$

where $\bar{\Psi}^2 = \sup_{t \geq 0} \|\Psi\|^2$, $\underline{p}, \bar{p} > 0$ are given by (26), and $\varepsilon > 0$ is given by (50).

Proof. See Appendix B.6. \square

Proposition 4 is a basic robustness result that provides some insights into the trade-offs involved in tuning the observer

gains α and γ with the objective of keeping $\hat{\theta}$ close to θ . In particular the result implies that

$$\|\hat{\theta} - \theta\|^2 \leq \varepsilon^{-1} \bar{p} (1 + \bar{\Psi}^2) r^2 \quad (35)$$

which we will now interpret in terms of the various types of structured uncertainty in the model.

1) *Time-varying parameters:* If there is no model mismatch, that is, $\bar{d}_v = 0$ and $\bar{d}_w = 0$, then (35) becomes

$$\|\hat{\theta} - \theta\|^2 \leq \bar{p} (1 + \bar{\Psi}^2) \lambda^{-2} (\bar{\Psi}^2 + \underline{p}^{-1}) \bar{d}_\theta^2$$

From (24a) and (25) we can see that the tracking error upper bound can be decreased by increasing the gain γ or increasing the excitation δ . Initially, increasing α is helpful since $\underline{p}^{-1} \propto \alpha^{-1}$ and λ can increase. However, \bar{p}^{-1} decreases exponentially with α and hence very large forgetting rates will lead to larger tracking errors. From this analysis, the forgetting factor should be selected large enough to allow tracking time-varying parameters, but not so large that it makes the system too sensitive to the unmodelled parameter dynamics.

2) *Model mismatch:* Suppose now that the unknown parameter is constant, that is, $\bar{d}_\theta = 0$. Now (35) yields

$$\|\hat{\theta} - \theta\|^2 \leq \bar{p} (1 + \bar{\Psi}^2) \lambda^{-2} (\bar{d}_v^2 + \varepsilon^{-1} \lambda_{\max}[M_w] \bar{d}_w^2)$$

Now we see that increasing α can only worsen the tracking of the true parameters. Furthermore, increasing γ is still beneficial, as it allows decreasing \bar{p} and increasing ε , as (50) shows. Finally, the stronger the contraction property of the internal dynamics, that is, the larger λ_w , the better for the estimation of time-varying parameters.

To conclude, notice that although increasing γ improves robustness to the unstructured uncertainty considered in this section, it in general degrades the performance of the observer when measurement errors are present (Section IV-B). This is a fundamental tradeoff in the observer design.

V. APPLICATION TO CONDUCTANCE-BASED MODELS

In this section we illustrate with numerical simulations how the system theoretic adaptive observers discussed in this paper perform when applied to problems in electrophysiology⁴.

A. Estimation of voltage and ion channel dynamics

Ion channels have been studied for a long time [14], and online databases such as ModelDB [31] now provide well-documented state-space models of the form (5) for many different types of ionic currents. Arbitrary neuron models can be postulated by connecting in parallel those readily available ionic current models. The primary goal of neuronal system identification is then to estimate the unknown model parameters: capacitances and maximal conductances [4], [10], [17], [32]. An important (and often ignored) point in this approach is the fact that the parameters in ionic channel models are only approximate in nature, and in practice may vary from neuron to neuron. Using the adaptive observer (27)-(28), in this section we illustrate a real-time solution to the problem of estimating the unknown and uncertain parameters of the Hodgkin-Huxley model of Examples 1 and 2.

⁴The Julia code used to generate these results can be found on <https://github.com/thiagoburghi/online-learning>.

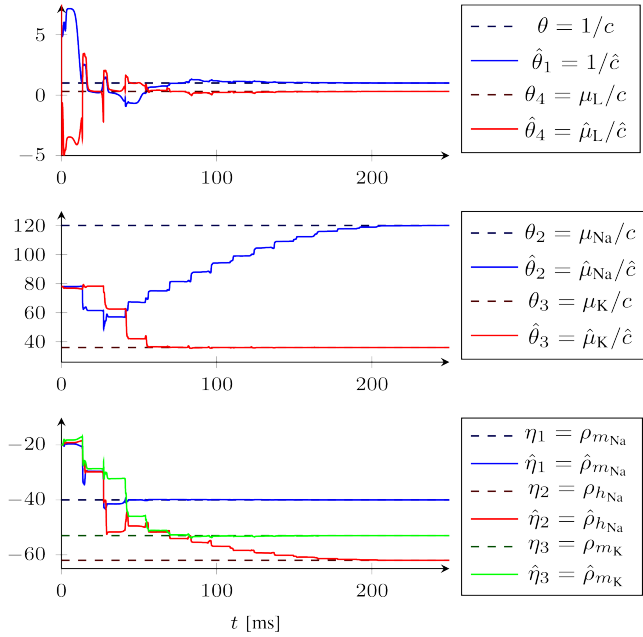


Fig. 5. Estimated parameters of the adaptive observer (27)-(28) in the estimation of the HH model when no measurement errors are present. Here, $\alpha = 0.1$ and $\beta = \gamma = 1$.

1) *Perfect measurements*: We begin by verifying the behaviour of the adaptive observer when no measurement errors are present. We use the output dynamics parameters in Table I, and the internal dynamics parameters in Appendix C.1. This results in

$$\begin{aligned}\theta(t) &= \theta(0) = (1, 120, 36, 0.3)^T \\ \eta(t) &= \eta(0) = (-40, -62, -53)^T\end{aligned}$$

By contrast, we initialize the observer with

$$\begin{aligned}\hat{\theta}(0) &= (2, 78, 78, 10)^T \\ \hat{\theta}_w(0) &= (-20, -20, -20)^T\end{aligned}$$

which represents a parsimonious guess over the parameters of an unknown and uncertain spiking conductance-based model. The true HH model and the adaptive observer were simulated subject to the input $u(t) = \sin(2\pi t/10)$ for $t \geq 0$. The initial conditions of the voltage and gating variables are given by $\text{col}(v(0), w(0)) = (-30, 0.5, 0.5, 0.5)^T$ and $\text{col}(\hat{v}(0), \hat{w}(0)) = (-30, 0, 0, 0)^T$ and the remaining initial conditions of the observer are given by $\Psi_v(0) = 0$, $\Psi_w(0) = 0$, $P(0) = I$. For $\alpha = 0.1$ and $\beta = \gamma = 1$, the solutions of the true system and of the adaptive observer can be seen in Figure 5. All the parameter estimates of the adaptive observer converge to the true parameter values.

2) *Measurement errors*: Keeping the same input and true system parameters used in the previous section, we now simulate the behaviour of the adaptive observer when zero-mean white Gaussian noise of variance $\sigma_{noise}^2 = 4 \text{ mV}^2$ is added to the measured v . Using the rms amplitude $v_{rms} \approx 27 \text{ mV}$ of the noise-free voltage trace simulated in the previous section, this noise corresponds to a relatively poor signal-to-noise-ratio of $10 \log_{10} v_{rms}^2 / \sigma_{noise}^2 \approx 22 \text{ dB}$. We first try using

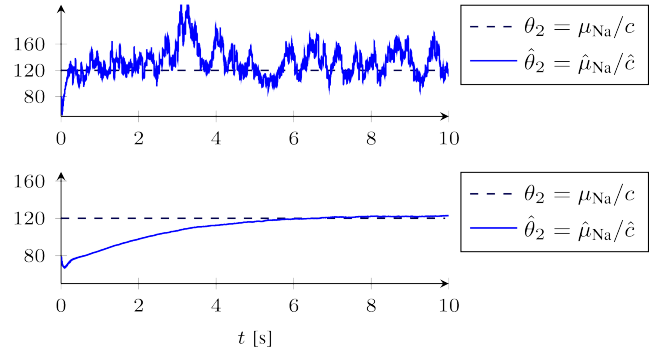


Fig. 6. Estimated parameters of the adaptive observer (27)-(28) in the estimation of the HH model when a white noise measurement error is present ($\sigma_{noise} = 2 \text{ mV}$). **Top**: $\alpha = 0.1$, $\beta = 1$, and $\gamma = 1$. **Bottom**: $\alpha = 10^{-4}$, $\beta = 1$, and $\gamma = 0.1$.

the same observer parameters $\alpha = 0.1$ and $\beta = \gamma = 1$ that previously led to convergence in the previous section. The result for the worst affected estimate, $\hat{\theta}_2$, is shown in Figure 6 (top). While the estimate remains bounded, it can be seen that the measurement noise considerably affects its convergence properties. However, tuning the observer parameters to $\alpha = 10^{-4}$, $\beta = 1$ and $\gamma = 0.1$ drastically improves the result, as shown in 6 (bottom). The oscillation in $\hat{\theta}_2(t)$ is now much less pronounced, and it converges more slowly to a region close to the true θ_2 . Similar behaviours hold for the less affected parameters. Comparing the two cases, there is a clear tradeoff between convergence rate and robustness to measurement noise.

B. Estimation of a neural circuit under neuromodulation

In this section, we illustrate the robustness to noise, model mismatch, and time-varying parameters by using the observer of Section IV-B to estimate the parameters θ of the HCO neuronal circuit introduced in Example 3.

Remark 8. When applied to a conductance-based network, choosing $\beta = 0$ makes the structure of the adaptive observers in this paper distributed, that is, the network observers decouple into n_v independent single neuron observers. This is because in a conductance-based network, Φ is block-diagonal and, by stability of the dynamics of Ψ in (24a) or (28a) and of $R := P^{-1}$ in (38), we can without loss of generality ignore all off-block diagonal terms of the matrices $\Psi(t)$ and $P(t)$.

Following Remark 8, applying the observer of Section IV-B to the HCO of Example 3 yields

$$\begin{aligned}\dot{\hat{v}}_i &= \varphi_i(\hat{v}_i, \hat{w}^{(i)})\hat{\mu}^{(i)} + c_i^{-1}u_i + \gamma(1 + \psi_i P_i \psi_i^T)(y_i - \hat{v}_i) \\ \dot{\hat{w}}^{(i)} &= A_i(y)\hat{w}^{(i)} + b(y, \hat{w}^{(i)}) \\ \dot{\hat{\mu}}^{(i)} &= \gamma P_i \psi_i^T (y_i - \hat{v}_i) \\ \dot{\psi}_i &= (-\gamma + \partial_{\hat{v}_i}[\varphi_i(\hat{v}_i, \hat{w}^{(i)})\varsigma(\hat{\mu}^{(i)})])\psi_i + \varphi_i(\hat{v}_i, \hat{w}^{(i)}), \\ \dot{P}_i &= \alpha P_i - \gamma P_i \psi_i^T \psi_i P_i\end{aligned}$$

where $P_i(0) \succ 0$, $i \in \mathcal{N} = \{1, 2\}$, and $y_i = v_i + e_i$. As in the previous section, we define the measurement errors e_1 and e_2 as white noise with $\sigma_{noise}^2 = 4 \text{ mV}^2$.

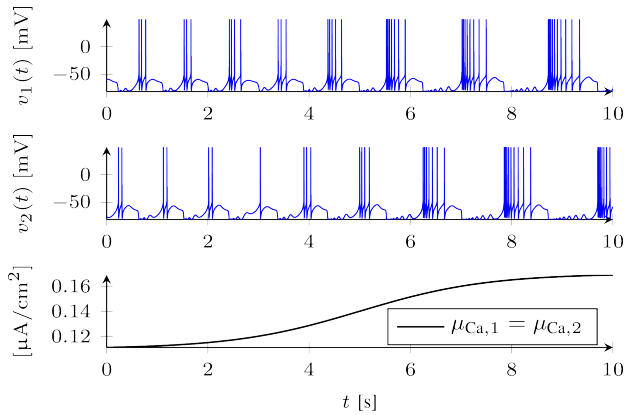


Fig. 7. True HCO voltage traces and time-varying calcium conductance used in Section V-B.

To illustrate the importance of tracking time-varying parameters, we consider the problem of neuromodulation [29]. Neuromodulators are substances that continuously modulate the opening of ion channels in a neuron's membrane. This modulatory control can be modelled as a temporal variation of the maximal conductances in a conductance-based model [9]. Here, we consider the case in which the calcium maximal conductances $\mu_{Ca,1}(t)$ and $\mu_{Ca,2}(t)$ of the true HCO model are slowly varied in time, something that is known to change the bursting frequency of the HCO model [6]. A gradual increase in the concentration of calcium ion channels is simulated by

$$\mu_{Ca(t),1}(t) = \mu_{Ca,2}(t) = 0.11 + \frac{0.07}{1 + \exp\left(-\frac{t-T_f/2}{1250}\right)} \quad (36)$$

where $T_f = 10$ seconds is the length of the simulation. For $i \in \{1, 2\}$, the remaining maximal conductances of the true HCO model are given by $\mu_{Na,i} = 60$, $\mu_{K,i} = 40$, $\mu_{L,i} = 0.035$, and $\mu_{G,2,1} = \mu_{G,1,2} = 4$.

In the observer above, the reversal potentials, capacitances, activation functions and time-constant functions are defined according to the nominal parameters of the true model detailed in Appendix C.2 (where initial conditions are also detailed). To simulate an unknown disturbance d_w in the true internal dynamics (see Section IV-C), a random disturbance of at most 1% (following the uniform distribution) is applied to every internal dynamics parameter of the true system.

Figure 7 illustrates the resulting voltage traces of the true (perturbed) HCO model. The neuromodulatory action on the calcium conductance increases the number of spikes in each burst. For a forgetting rate of $\alpha = 0.0025$, observer gains of $\beta = 0$ and $\gamma = 0.1$, and a constant input $u_1(t) = u_2(t) = -0.65 \mu\text{A}/\text{cm}^2$, Figure 8 shows the trajectories of some of the true and estimated maximal conductances. It can be seen that the estimates converge towards a region close to the true parameters, illustrating the robustness of the convergence property of the observer. The bias in the estimates after convergence is expected, as the internal dynamics of the observer and of the true model are different due to model mismatch (but simulating the estimated model with fixed $\hat{\theta}(t = 10\text{s})$ results in half-center oscillations congruent with the those

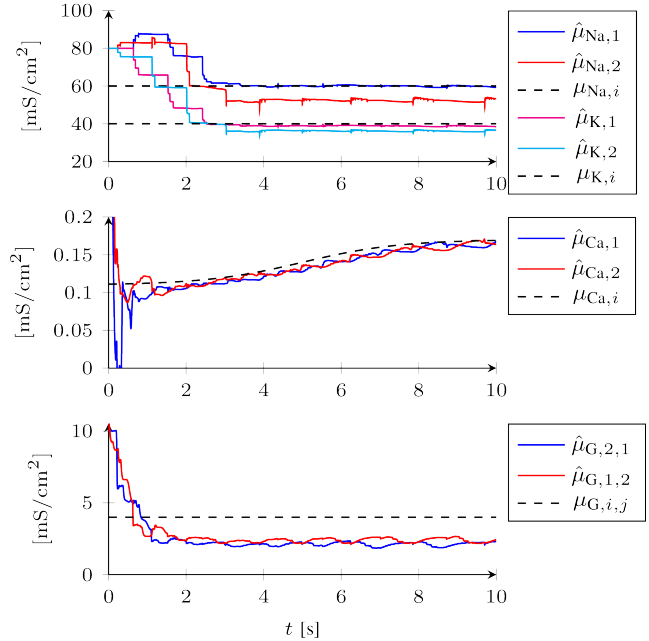


Fig. 8. Example trajectories of HCO maximal conductance estimates when noise and model mismatch are present (see Section V-B).

of the true system). The calcium conductance estimates track the true calcium conductances by remaining in a time-varying region around the true value. A comparison with Figure 7 shows that calcium estimates are corrected whenever a burst of spikes is elicited. Each burst can thus be seen as providing a very rich signal for the observer to update its estimates.

VI. CONCLUDING REMARKS

We have presented an adaptive observer which can be used for real-time estimation of conductance-based models of neuronal circuits. The observers in this work can be used for indirect adaptive control of neuronal maximal conductances [41], opening the way for innovative neurophysiology research using dynamic clamp protocols [43].

VII. ACKNOWLEDGEMENTS

We thank Dr Fulvio Forni and Raphael Schmetterling for the feedback given during the writing of this manuscript. We also thank the anonymous reviewers who greatly contributed to the improvement of the results.

APPENDIX

A. Contraction analysis

The system dynamics

$$\dot{x} = f(x, u) \quad (37)$$

is said to be *exponentially contracting* [25] in x on $X \subset \mathbb{R}^{n_x}$, uniformly in u on $U \subseteq \mathbb{R}^{n_u}$, if there exist a continuously differentiable symmetric matrix $P(x, t)$, called the *contraction metric*, and a constant $\lambda > 0$, called the *contraction rate*, such that $\epsilon_1 I \preceq P(x, t) \preceq \epsilon_2 I$ for some $\epsilon_1, \epsilon_2 > 0$, and

$\partial_x f^\top P + P \partial_x f + \dot{P} \preceq -\lambda P$ for all $t \geq 0$, all $x \in X$, and all $u \in U$. The set $X \subset \mathbb{R}^{n_x}$ is said to be *positively invariant* with respect to the dynamics (37), uniformly in u on $U \subseteq \mathbb{R}^{n_u}$, if $x(0) \in X$ and $u(t) \in U$ for all $t \geq 0$ imply $x(t) \in X$ for all $t \geq 0$. It is a well-known fact that if the dynamics (37) are exponentially contracting on a convex positively invariant set X , then all solutions of that system starting in X converge towards each other exponentially fast, with rate λ (for a proof of this statement, see for instance [19, Lemma 1]).

B. Proofs

1) *Proof of Lemma 1:* We begin by noticing that $[0, 1]$ is a positively invariant set for (5b) and for (5c), uniformly in v on \mathbb{R} . This is because the image of the sigmoid (6) is $(0, 1)$, which implies none of the gating variables m_{ion} and h_{ion} can leave the set $[0, 1]$: for instance, $\dot{m}_{\text{ion}} \geq 0$ for $m_{\text{ion}} = 0$ and all $v \in \mathbb{R}$, and $\dot{m}_{\text{ion}} \leq 0$ for $m_{\text{ion}} = 1$ and all $v \in \mathbb{R}$. Now, assuming $m_{\text{ion}}(0) \in [0, 1]$ and $h_{\text{ion}}(0) \in [0, 1]$, we have $\mu_{\text{ion}} m_{\text{ion}}^{p_{\text{ion}}} h_{\text{ion}}^{q_{\text{ion}}} > 0$ for all $\text{ion} \in \mathcal{I}$ and all $t \geq 0$. This in turn implies v cannot leave the interval $[\underline{v}, \bar{v}]$, which can be verified by inspection of (3)-(5a): if $v = \bar{v}$, then $\dot{v} \leq 0$, whereas if $v = \underline{v}$, then $\dot{v} \geq 0$.

2) *Proof of Proposition 3:* The normal equation of the LS problem (19)-(22) with $R_0(T) = e^{-\alpha T} P^{-1}(0)/T$ is

$$R(T)\hat{\theta}(T) = \int_0^T e^{-\alpha(T-\tau)} \Psi(\tau)^\top (H\dot{v}(\tau) - H\hat{a}(\tau)) d\tau$$

where

$$R(t) = e^{-\alpha t} P^{-1}(0) + \gamma \int_0^t e^{-\alpha(t-\tau)} \Psi(\tau)^\top \Psi(\tau) d\tau \quad (38)$$

Differentiating the normal equation by T and evaluating at t we obtain the RLS solution

$$\dot{\hat{\theta}}(t) = P(t)\Psi(t)^\top (H\dot{v}(t) - \gamma\Psi(t)\hat{\theta}(t) - H\hat{a}(t))$$

Thus (23)-(24) implements the RLS solution if and only if

$$H\dot{v}(t) - \gamma\Psi(t)\hat{\theta}(t) - H\hat{a}(t) = \gamma(v(t) - \hat{v}(t)) \quad (39)$$

To verify the above identity, we first notice that

$$\begin{aligned} \frac{d}{dt}(\Psi\hat{\theta}) &= -\gamma\Psi\hat{\theta} + \Phi\hat{\theta} + \gamma\Psi P\Psi^\top(v - \hat{v}) \\ &= -\gamma\Psi\hat{\theta} + \dot{\hat{v}} - \gamma(v - \hat{v}) - \hat{a} \end{aligned}$$

Solving the previous equation for $\Psi\hat{\theta}$ and multiplying the result by γ , we obtain

$$\gamma\Psi(t)\hat{\theta}(t) = -\gamma H v(t) - H\hat{a}(t) + \gamma\hat{v}(t)$$

We can now recover (39) by adding $\gamma(v(t) - \hat{v}(t))$ to both sides of the previous equation and applying the identity

$$\gamma(v(t) - H v(t)) = H\dot{v}(t)$$

which can be easily verified from (21).

3) *Proof of Lemma 3:* Consider the system

$$\dot{R} = -\alpha R + \gamma\Psi^\top\Psi \quad (40)$$

with $R(0) = P(0)^{-1} \succ 0$, whose solution is given by (38). Our assumptions imply that $\bar{p}^{-1}I \preceq R(t) \preceq \underline{p}^{-1}I$, in which case $R(t)$ is uniformly invertible and $P(t) = \bar{R}(t)^{-1}$ follows from the identity $\dot{R} = \dot{P}^{-1} = -P^{-1}\dot{P}P^{-1}$. Indeed, the lower bound $\bar{p}^{-1}I$ of $R(t)$, given by (25), is derived as in the proof of [51, Lemma 1]. The upper bound $\underline{p}^{-1}I$ of $R(t)$ exists due to the boundedness of Ψ , which can be established directly from (24a) and boundedness of Φ (Remark 1).

4) *Proof of Theorem 1:* We prove this result using the *virtual system* idea of contraction analysis [25], [49]: we construct a so-called virtual system whose solutions contain the solutions of both (14) and (23); then we show that the virtual system is globally exponentially contracting; this will imply that any solutions of (14) and (23) converge exponentially fast towards each other. We consider the virtual state vector

$$\tilde{x} = \text{col}(\tilde{v}, \tilde{w}, \tilde{\theta})$$

and the virtual system given by

$$\begin{aligned} \dot{\tilde{v}} &= \tilde{f}(t, \tilde{w}, \tilde{\theta}) + \gamma(I + \Psi P \Psi^\top)(v - \tilde{v}) \\ \dot{\tilde{w}} &= A(v)\tilde{w} + b(v) \\ \dot{\tilde{\theta}} &= \gamma P \Psi^\top(v - \tilde{v}) \end{aligned} \quad (41)$$

where

$$\tilde{f}(t, \tilde{w}, \tilde{\theta}) = \Phi(v, \tilde{w}, u)\theta + \Phi(v, \hat{w}, u)(\tilde{\theta} - \theta) + a(v, \tilde{w}, u)$$

By construction of $\tilde{f}(t, \tilde{w}, \tilde{\theta})$, any solutions $x = \text{col}(v, w, \theta)$ of (14) and $\hat{x} = \text{col}(\hat{v}, \hat{w}, \hat{\theta})$ of (23) are particular solutions of the virtual system (41); notice that $v(t)$, $\hat{w}(t)$, and $u(t)$ are not states of the virtual system.

To show that the virtual system is globally exponentially contracting, we use the differential Lyapunov function

$$\delta V(t, \delta\tilde{x}) = \delta\tilde{x}^\top T(t)^\top \bar{M}(t) T(t) \delta\tilde{x} \quad (42)$$

where

$$T = \begin{bmatrix} I & 0 & -\Psi \\ 0 & I & 0 \\ 0 & 0 & I \end{bmatrix}, \quad \bar{M} = \begin{bmatrix} \varepsilon I & 0 & 0 \\ 0 & M_w & 0 \\ 0 & 0 & \varepsilon P^{-1} \end{bmatrix} \quad (43)$$

and $\delta\tilde{x}$ is the state vector of the differential system $\delta\dot{\tilde{x}} = J\delta\tilde{x}$, with

$$J = \begin{bmatrix} -\gamma(I + \Psi P \Psi^\top) & \partial_{\tilde{w}}\tilde{f}(t, \tilde{w}, \tilde{\theta}) & \Phi(v, \hat{w}, u) \\ 0 & A(v) & 0 \\ -\gamma P \Psi^\top & 0 & 0 \end{bmatrix} \quad (44)$$

the Jacobian of the vector field of (41). It can easily be verified that

$$\delta\dot{V}(t, \delta\tilde{x}, \tilde{x}) = \delta\tilde{x}^\top T(t)^\top \left(\bar{J}^\top \bar{M} + \bar{M} \bar{J} + \dot{\bar{M}} \right) T(t) \delta\tilde{x} \quad (45)$$

where

$$\bar{J} = (TJ + \dot{T})T^{-1} \quad (46)$$

Hence to show global contraction we must show that

$$M := T^\top \bar{M} T = \begin{bmatrix} \varepsilon I & 0 & -\varepsilon\Psi \\ 0 & M_w & 0 \\ -\varepsilon\Psi^\top & 0 & \varepsilon(\Psi^\top\Psi + P^{-1}) \end{bmatrix} \quad (47)$$

is uniformly positive definite, and that there is $\lambda > 0$ such that

$$\bar{J}^T \bar{M} + \bar{M} \bar{J} + \dot{\bar{M}} \preceq -\lambda \bar{M} \quad (48)$$

for all $\tilde{x} \in \mathbb{R}^{n_v+n_w+n_\theta}$ and $t \geq 0$. Uniform positive definiteness of M can be shown using Lemma 3 and boundedness of $\Psi(t)$. Indeed, by Remark 1 and stability of (24b), $\Psi(t)$ is bounded; let $\bar{\Psi}^2 = \sup_{t \geq 0} \|\Psi(t)\|^2$. Then it can be verified with Schur's complement that

$$M(t) \succeq \text{diag} \left(\frac{\varepsilon \bar{p}^{-1}}{1 + \bar{p}^{-1} + \bar{\Psi}^2} I, \lambda_{\min}[M_w] I, \frac{\varepsilon \bar{p}^{-1}}{1 + \bar{\Psi}^2} I \right) \quad (49)$$

for all $t \geq 0$. Now computing the left-hand side of (48) from (43), (44), and (46), we obtain

$$\bar{J}^T \bar{M} + \bar{M} \bar{J} + \dot{\bar{M}} = \begin{bmatrix} -2\varepsilon\gamma I & \varepsilon \partial_{\tilde{w}} \tilde{f}(t, \tilde{w}, \tilde{\theta}) & -\gamma \varepsilon \Psi \\ * & A(v)^T M_w + M_w A(v) & 0 \\ * & * & -\varepsilon(\gamma \Psi \Psi^T + \alpha P^{-1}) \end{bmatrix} \preceq Q$$

Where the upper bound matrix Q is given by

$$Q = \begin{bmatrix} -\varepsilon\gamma I & \varepsilon \partial_{\tilde{w}} \tilde{f}(t, \tilde{w}, \tilde{\theta}) & 0 \\ * & -\lambda_w M_w & 0 \\ * & * & -\varepsilon \alpha P^{-1} \end{bmatrix}$$

Finally, notice that

$$\partial_{\tilde{w}} \tilde{f}(t, \tilde{w}, \tilde{\theta}) = \partial_{\tilde{w}} (\Phi(v, \tilde{w}, u)\theta + a(v, \tilde{w}, u))$$

is bounded (Remark 1). Thus for any $\lambda < \min\{\alpha, \lambda_w, \gamma\}$ choosing

$$\varepsilon < (\lambda_w - \lambda)(\gamma - \lambda) \lambda_{\min}[M_w] \sup \|\partial_{\tilde{w}} \tilde{f}(t, \tilde{w}, \tilde{\theta})\|^{-2} \quad (50)$$

ensures $Q \preceq -\lambda \bar{M}$ and hence (48) holds globally, and the virtual system is globally exponentially contracting.

5) Proof of Theorem 2: In similar fashion to the proof of Theorem 1, we begin by considering the virtual state vector

$$\tilde{x} := \text{col}(\tilde{v}, \tilde{w}, \text{col}(\tilde{\theta}, \tilde{\eta}))$$

and the virtual system

$$\begin{aligned} \dot{\tilde{v}} &= \tilde{f}(t, \tilde{w}, \tilde{\theta}) + \gamma(I + \Psi_v P \Psi_v^T)(v - \tilde{v}) \\ \dot{\tilde{w}} &= \tilde{g}(t, \tilde{w}, \tilde{\theta}) + \gamma \Psi_w P \Psi_w^T (v - \tilde{v}) \\ \text{col}(\dot{\tilde{\theta}}, \dot{\tilde{\eta}}) &= \gamma P \Psi_v^T (v - \tilde{v}) \end{aligned} \quad (51)$$

where

$$\begin{aligned} \tilde{f}(t, \tilde{w}, \tilde{\theta}) &= \Phi(v, \tilde{w}, u)\theta + \Phi(v, \hat{w}, u)(\tilde{\theta} - \theta) + a(v, \tilde{w}, u) \\ \tilde{g}(t, \tilde{w}, \tilde{\eta}) &= A(v, \tilde{\eta})w + A(v, \hat{\eta})(\tilde{w} - w) + b(v, \tilde{\eta}) \end{aligned}$$

Notice that by construction of \tilde{f} and \tilde{g} , any solutions $x = \text{col}(v, w, \theta, \eta)$ of (1) and $\hat{x} = \text{col}(\hat{v}, \hat{w}, \hat{\theta}, \hat{\eta})$ of (27) are particular solutions of the virtual system (51). We use the differential Lyapunov equation $\partial V = \partial \tilde{x}^T T^T \bar{M} T \partial \tilde{x} := \partial \tilde{x}^T M \partial \tilde{x}$, with T and \bar{M} given by

$$T = \begin{bmatrix} I & -\Psi \\ 0 & I \end{bmatrix}, \quad \bar{M} = \begin{bmatrix} \varepsilon I & 0 & 0 \\ 0 & M_w & 0 \\ 0 & 0 & \varepsilon P^{-1} \end{bmatrix}, \quad (52)$$

and $\delta \tilde{x}$ the state of the differential system $\delta \dot{\tilde{x}} = J \delta \tilde{x}$ (we shall use lines to delimit block sub-matrices of the same size). The Jacobian J of the vector field of (51) is given by

$$J = \left[\begin{array}{cc|cc} -\gamma \Psi P \Psi_v^T & 0 & 0 & 0 \\ -\gamma P \Psi_v^T & 0 & 0 & 0 \end{array} \right] + \left[\begin{array}{c|c} \tilde{A}_\Psi(t) & \tilde{B}_\Psi(t) \\ \hline 0 & 0 \end{array} \right] \quad (53)$$

where

$$\begin{aligned} \tilde{A}_\Psi(t) &= \begin{bmatrix} -\gamma I & \partial_{\tilde{w}} [\Phi(v, \tilde{w}, u)\theta + a(v, \tilde{w}, u)] \\ 0_{n_w \times n_v} & A(v, \hat{\eta}) \end{bmatrix} \\ \tilde{B}_\Psi(t) &= \begin{bmatrix} \Phi(v, \hat{w}, u) & 0_{n_v \times n_\eta} \\ 0_{n_w \times n_\theta} & \partial_{\tilde{\eta}} [A(v, \hat{\eta})w + b(v, \hat{\eta})] \end{bmatrix} \end{aligned}$$

It can be verified that the metric

$$M = \begin{bmatrix} \varepsilon I & 0 & -\varepsilon \Psi_v \\ 0 & M_w & -M_w \Psi_w \\ -\varepsilon \Psi_v^T & -M_w \Psi_w^T & \varepsilon (\Psi_v^T \Psi_v + P^{-1}) + \Psi_w M_w \Psi_w \end{bmatrix}$$

is uniformly positive definite and bounded. Indeed, our assumptions imply that the dynamics of Ψ in (28a) is globally exponentially contracting, while $B_\Psi(t)$ is bounded (see Remarks 1 and 4). Hence, $\Psi = \text{col}(\Psi_v, \Psi_w)$ is bounded, and since P is uniformly bounded, Schur's complement can be used to show that (49) also holds for M above.

As in the previous proof, $\partial \dot{V}(t, \partial \tilde{x}, \tilde{x})$ satisfies (45), with \bar{J} given by (46) but J now given by (53) and T given by (52). Computing \bar{J} while replacing $\tilde{\Psi}$ by (28a) we obtain

$$\bar{J} = \left[\begin{array}{c|c} \tilde{A}_\Psi(t) & \left(\tilde{A}_\Psi(t) - A_\Psi(t) \right) \Psi + \tilde{B}_\Psi(t) - B_\Psi(t) \\ \hline -\gamma P \Psi_v^T & 0 \end{array} \right] \begin{array}{c} \\ \\ \\ -\gamma P \Psi_v^T \Psi_v \end{array}$$

Computing the left-hand side of (48) from (52) and \bar{J} above, we obtain

$$\bar{J}^T \bar{M} + \bar{M} \bar{J} + \dot{\bar{M}} \preceq Q$$

where the upper bound matrix $Q = Q^T$ is now given by

$$Q = \left[\begin{array}{cc|cc} -\gamma \varepsilon I & \varepsilon \partial_{\tilde{w}} \tilde{f}(t, \tilde{w}, \tilde{\theta}) & 0 & \varepsilon \Delta_1 \Psi_{w,2} \\ * & -\lambda_w M_w & 0 & M_w \Delta_2 \\ \hline * & * & -\varepsilon (\alpha P^{-1} + \beta P^{-2}) & \end{array} \right]$$

where we used $\Psi_w = [0 \quad \Psi_{w,2}]$ (see Remark 6). Here,

$$\begin{aligned} \Delta_1 &= \partial_{\tilde{w}} [\Phi(v, \tilde{w}, u)\theta + a(v, \tilde{w}, u)] - \partial_{\hat{w}} [\Phi(v, \hat{w}, u)\theta + a(v, \hat{w}, u)] \\ &\quad + \partial_{\hat{w}} [\Phi(v, \hat{w}, u)(\theta - \varsigma_\theta(\hat{\theta}))] \end{aligned} \quad (54a)$$

and

$$\begin{aligned} \Delta_2 &= \partial_{\tilde{\eta}} [A(v, \tilde{\eta})w + b(v, \tilde{\eta})] - \partial_{\hat{\eta}} [A(v, \hat{\eta})w + b(v, \hat{\eta})] \\ &\quad + \partial_{\hat{\eta}} [A(v, \hat{\eta})(w - \varsigma_w(\hat{w}))] \end{aligned} \quad (54b)$$

We now show that for any $\lambda < \min\{\alpha, \lambda_w, \gamma\}$, $Q \preceq -\lambda \bar{M}$ holds locally around \hat{x} . Choosing ε as in (50) yields

$$-Q - \lambda \bar{M} \succeq \begin{bmatrix} \varepsilon(\gamma - \lambda)I & 0 & 0 & -\varepsilon \Delta_1 \Psi_{w,2} \\ * & (\lambda_w - \lambda)M_w & 0 & -M_w \Delta_2 \\ \hline * & * & \varepsilon((\alpha - \lambda)P^{-1} + \beta P^{-2}) & \end{bmatrix}$$

and hence it follows from Schur's complement that the right-hand side of the inequality above is positive semidefinite if and only if

$$\varepsilon((\alpha - \lambda)P^{-1} + \beta P^{-2}) \succeq \begin{bmatrix} 0 & 0 \\ 0 & \varepsilon \frac{\Psi_{w,2}^\top \Delta_1^\top \Delta_1 \Psi_{w,2}}{\gamma - \lambda} + \frac{\Delta_2^\top M_w \Delta_2}{\lambda_w - \lambda} \end{bmatrix}$$

By an argument similar to that of [3, Proposition 3], by continuity and by the global Lipschitz properties of Δ_1 and Δ_2 in (54), as well as by boundedness of $\Psi_{w,2}$, it follows that there exists a number $r > 0$ such that for all $x(t)$ and \tilde{x} satisfying $\|x(t) - \hat{x}(t)\| \leq r$ and $\|\tilde{x} - \hat{x}(t)\| \leq r$ for all $t \geq 0$, we have

$$\varepsilon \frac{\|\Delta_1 \Psi_{w,2}\|^2}{\gamma - \lambda} + \frac{\|M_w^{\frac{1}{2}} \Delta_2\|^2}{\lambda_w - \lambda} \leq \varepsilon((\alpha - \lambda)\underline{p}^{-1} + \beta \underline{p}^{-2})$$

and hence $Q \preceq -\lambda M$ for all $t \geq 0$. Hence as long as $\|x(t) - \hat{x}(t)\| \leq r$ for all $t \geq 0$, any solution $\tilde{x}(t)$ of the virtual system whose initial condition satisfies $\|\tilde{x}(0) - \hat{x}(0)\|_{M(0)} \leq r \underline{m}$ will also satisfy $\|\tilde{x}(t) - \hat{x}(t)\|_{M(t)} \leq r \underline{m}$ and will contract to the trajectory $\hat{x}(t)$ exponentially fast as $t \rightarrow \infty$. But $x(t)$ is a valid trajectory of the virtual system; hence $\|x(0) - \hat{x}(0)\|_{M(0)} \leq r \underline{m}$ implies that $\|x(t) - \hat{x}(t)\| \leq r$ for all $t \geq 0$ and that $x(t)$ contracts towards $\hat{x}(t)$. Hence $\hat{x}(t) \rightarrow x(t)$ exponentially fast as $t \rightarrow \infty$, with rate λ .

6) *Proof of Proposition 4*: The proof follows the ideas in [3], [5]. Consider the *nominal* virtual system

$$\dot{\tilde{x}} = F(t, \tilde{x}) \quad (55)$$

where F is given by the right-hand side of (41) and $\tilde{x} = \text{col}(\tilde{v}, \tilde{w}, \tilde{\theta})$ are the virtual states. Consider also the *perturbed* virtual system

$$\dot{\tilde{x}}_d = F(t, \tilde{x}_d) + d(t, \tilde{x}_d) \quad (56)$$

where $\tilde{x}_d = \text{col}(\tilde{v}_d, \tilde{w}_d, \tilde{\theta}_d)$ and $d(t, \tilde{x}_d)$ is the perturbation vector field from (32). In Appendix B.4, we have shown that (55) is globally exponentially contracting, with a uniformly positive definite contraction metric $M = T^\top \bar{M} T$ given by (47), and a contraction rate given by $\lambda < \min\{\alpha, \lambda_w, \gamma\}$. Following [25, Section 3.7 (vii)], contraction of (55) implies that

$$\|\tilde{x}_d(t) - \tilde{x}(t)\|_{M(t)} \leq e^{-\lambda t} \|\tilde{x}_d(0) - \tilde{x}(0)\|_{M(0)} + \tilde{d}(t) \quad (57)$$

for all $t \geq 0$, with

$$\tilde{d}(t) = \int_0^t e^{-\lambda(t-\tau)} \|d(\tau, \tilde{x}_d(\tau))\|_{M(\tau)} d\tau \quad (58)$$

The result will follow from the asymptotic behaviour of the inequality (57). To derive an upper bound for (57), we have

$$\begin{aligned} \|d\|_M^2 &= \|T d\|_{\bar{M}}^2 = \varepsilon \|d_v - \Psi d_\theta\|^2 + \|d_w\|_{M_w}^2 + \varepsilon \|d_\theta\|_{P^{-1}}^2 \\ &\leq \varepsilon \|d_v\|^2 + \|d_w\|_{M_w}^2 + \varepsilon \|d_\theta\|_{\Psi^\top \Psi + P^{-1}}^2 \end{aligned}$$

for all $t \geq 0$, and hence from Assumption 7 and (58) we obtain $\tilde{d}(t) \leq \sqrt{r}$ with r given by (34). Then, from the lower bound of $M(t)$ in (49), we have

$$\|\tilde{x}_d - \tilde{x}\|_D^2 \leq \|\tilde{x}_d - \tilde{x}\|_{M(t)}^2$$

with D given by (33). It follows from (57) and the above bounds that

$$\|\tilde{x}_d - \tilde{x}\|_D \leq e^{-\lambda t} \|\tilde{x}_d(0) - \tilde{x}(0)\|_{M(0)} + \sqrt{r}$$

The inequality above shows that any solution $\tilde{x}(t)$ of the nominal virtual system (55) converges exponentially fast towards the ball $\mathcal{B}_{r,D}(\tilde{x}_d(t))$, where $\tilde{x}_d(t)$ is any solution of the perturbed virtual system (56). Now, we have that $x(t)$ is a particular solution of the perturbed virtual system (56). In addition, $\hat{x}(t)$ is a particular solution of the exponentially contracting nominal virtual system (55), and thus it converges exponentially fast towards any other solution $\tilde{x}(t)$. Thus, $\hat{x}(t)$ converges exponentially fast towards $\mathcal{B}_{r,D}(x(t))$.

C. Model parameters

1) *Hodgkin-Huxley model*: HH model parameters were adapted from [18, pp. 46-47]. All activation functions are of the form (6), and all time-constant functions are of the form (7), with parameters given in the table below:

	ρ	κ	$\underline{\tau}$	$\bar{\tau}$	ζ	χ
m_{Na}	-40	9	0.04	0.50	-38	30
h_{Na}	-62	-7	1.2	8.6	-67	20
m_{K}	-53	15	1.1	5.8	-79	50

2) *Half-center oscillator*: Both neurons in the HCO of Section V-B have identical nominal capacitances, reversal potentials and internal dynamics. The reversal potentials are given by $\nu_{\text{Na}} = 50$, $\nu_{\text{K}} = \nu_{\text{G}} = -80$, $\nu_{\text{Ca}} = 120$, and $\nu_{\text{L}} = -49$ mV; the capacitances are given by $c_1 = c_2 = 1$. The internal dynamics were adapted from [6, p.2474]. All activation functions are of the form (6), and all intrinsic time-constant functions are of the form (7), with parameters given in the table below. The synaptic time-constant (11) has $a_{\text{G}} = 2$ and $b_{\text{G}} = 0.1$.

	ρ	κ	$\underline{\tau}$	$\bar{\tau}$	ζ	χ
m_{Na}	-35.5	5.29	0.06	42.37	-387.92	133.78
h_{Na}	-48.9	-5.18	1.50	2.50	-62.90	10.00
m_{K}	-12.3	11.8	0.80	6.65	-76.62	61.42
m_{Ca}	-67.1	7.20	1.01	40.03	-117.58	62.87
h_{Ca}	-82.1	-5.5	40.49	126.51	-92.48	-50.24
s_{G}	-45	2	-	-	-	-

We have chosen the HCO initial conditions $v(0)$ and $w(0)$ from the trajectory observed at steady-state oscillations with $\mu_{\text{Ca},1} = \mu_{\text{Ca},2} = 0.11$. The adaptive observer initial conditions were arbitrarily set to $\hat{v}(0) = (-50, -50)^\top$, $\hat{w}^{(1)}(0) = \hat{w}^{(2)}(0) = 0$, $\hat{\mu}_{\text{Na},1}(0) = \hat{\mu}_{\text{Na},2}(0) = 80$, $\hat{\mu}_{\text{K},1}(0) = \hat{\mu}_{\text{K},2}(0) = 80$, $\hat{\mu}_{\text{Ca},1}(0) = \hat{\mu}_{\text{Ca},2}(0) = 1$, $\hat{\mu}_{\text{L},1}(0) = \hat{\mu}_{\text{L},2}(0) = 1$, $\hat{\mu}_{\text{G},1,1}(0) = \hat{\mu}_{\text{G},1,2}(0) = 10$, $\psi^{(1)}(0) = \psi^{(2)}(0) = 0$, and $P^{(1)}(0) = P^{(2)}(0) = I$.

REFERENCES

- [1] Henry D. I. Abarbanel, Daniel R. Creveling, and James M. Jeanne. Estimation of parameters in nonlinear systems using balanced synchronization. *Physical Review E*, 77(1), January 2008.

- [2] Gildas Besançon. Remarks on nonlinear adaptive observer design. *Systems & Control Letters*, 41(4):271–280, November 2000.
- [3] Silvere Bonnabel and Jean-Jacques Slotine. A Contraction Theory-Based Analysis of the Stability of the Deterministic Extended Kalman Filter. *IEEE Transactions on Automatic Control*, 60(2):565–569, February 2015.
- [4] Thiago B. Burghi, Maarten Schoukens, and Rodolphe Sepulchre. Feedback identification of conductance-based models. *Automatica*, 123:109297, January 2021.
- [5] Domitilla Del Vecchio and Jean-Jacques E. Slotine. A Contraction Theory Approach to Singularly Perturbed Systems. *IEEE Transactions on Automatic Control*, 58(3):752–757, March 2013.
- [6] Julie Dethier, Guillaume Drion, Alessio Franci, and Rodolphe Sepulchre. A positive feedback at the cellular level promotes robustness and modulation at the circuit level. *Journal of Neurophysiology*, 114(4):2472–84, October 2015.
- [7] G. Drion, T. O’Leary, J. Dethier, A. Franci, and R. Sepulchre. Neuronal behaviors: A control perspective. In *54th IEEE Conference on Decision and Control*, pages 1923–1944, December 2015.
- [8] Guillaume Drion, Julie Dethier, Alessio Franci, and Rodolphe Sepulchre. Switchable slow cellular conductances determine robustness and tunability of network states. *PLOS Computational Biology*, 14(4):e1006125, April 2018.
- [9] Guillaume Drion, Alessio Franci, and Rodolphe Sepulchre. Cellular switches orchestrate rhythmic circuits. *Biological Cybernetics*, 113(1):71–82, April 2019.
- [10] Shaul Druckmann, Yoav Banitt, Albert Gidon, Felix Schürmann, Henry Markram, and Idan Segev. A Novel Multiple Objective Optimization Framework for Constraining Conductance-Based Neuron Models by Experimental Data. *Frontiers in Neuroscience*, 1(1):7–18, October 2007.
- [11] G. Bard Ermentrout and David H. Terman. *Mathematical Foundations of Neuroscience*. Springer, New York, 2010.
- [12] M. Farza, M. M’Saad, T. Maatoug, and M. Kamoun. Adaptive observers for nonlinearly parameterized class of nonlinear systems. *Automatica*, 45(10):2292–2299, October 2009.
- [13] J.P. Gauthier, H. Hammouri, and S. Othman. A simple observer for nonlinear systems applications to bioreactors. *IEEE Transactions on Automatic Control*, 37(6):875–880, June 1992.
- [14] Bertil Hille. *Ionic channels of excitable membranes*. Sinauer Associates, Sunderland, MA, 1984.
- [15] A. L. Hodgkin and A. F. Huxley. A quantitative description of membrane current and its application to conduction and excitation in nerve. *The Journal of Physiology*, 117(4):500–544, August 1952.
- [16] A. L. Hodgkin, A. F. Huxley, and B. Katz. Measurement of current-voltage relations in the membrane of the giant axon of Loligo. *The Journal of Physiology*, 116(4):424–448, April 1952.
- [17] Quentin J. M. Huys, Misha B. Ahrens, and Liam Paninski. Efficient Estimation of Detailed Single-Neuron Models. *Journal of Neurophysiology*, 96(2):872–890, August 2006.
- [18] Eugene M. Izhikevich. *Dynamical Systems in Neuroscience*. MIT Press, Cambridge, MA, 2007.
- [19] Jerome Jouffroy and Thor I. Fossen. A Tutorial on Incremental Stability Analysis using Contraction Theory. 31(3):93–106, July 2010.
- [20] James Keener and James Sneyd. *Mathematical Physiology*, volume 8/1. Springer, New York, NY, 2 edition, 2009.
- [21] Thomas Knöpfel and Chenchen Song. Optical voltage imaging in neurons: moving from technology development to practical tool. *Nature Reviews Neuroscience*, 20(12):719–727, December 2019.
- [22] Miroslav Krstic, Petar V. Kokotovic, and Ioannis Kanellakopoulos. *Nonlinear and Adaptive Control Design*. John Wiley & Sons, Inc., New York, 1st edition, 1995.
- [23] L. Ljung. Convergence analysis of parametric identification methods. *IEEE Transactions on Automatic Control*, 23(5):770–783, October 1978.
- [24] Lennart Ljung. *System Identification: Theory for the User*. Prentice Hall PTR, Upper Saddle River, NJ, 1999.
- [25] Winfried Lohmiller and Jean-Jacques E. Slotine. On Contraction Analysis for Non-linear Systems. *Automatica*, 34(6):683–696, June 1998.
- [26] Brett T. Lopez and Jean-Jacques E. Slotine. Adaptive Nonlinear Control With Contraction Metrics. *IEEE Control Systems Letters*, 5(1):205–210, January 2021.
- [27] I. R. Manchester, M. M. Tobenkin, and J. Wang. Identification of nonlinear systems with stable oscillations. In *2011 50th IEEE Conference on Decision and Control and European Control Conference*, pages 5792–5797, Orlando, FL, December 2011.
- [28] Eve Marder and Dirk Bucher. Central pattern generators and the control of rhythmic movements. *Current Biology*, 11(23):R986–R996, November 2001.
- [29] Eve Marder, Timothy O’Leary, and Sonal Shruti. Neuromodulation of Circuits with Variable Parameters: Single Neurons and Small Circuits Reveal Principles of State-Dependent and Robust Neuromodulation. *Annual Review of Neuroscience*, 37(1):329–346, 2014.
- [30] R. Marino and P. Tomei. Global adaptive observers for nonlinear systems via filtered transformations. *IEEE Transactions on Automatic Control*, 37(8):1239–1245, August 1992. Conference Name: IEEE Transactions on Automatic Control.
- [31] Robert A. McDougal, Thomas M. Morse, Ted Carnevale, Luis Marengo, Rixin Wang, Michele Migliore, Perry L. Miller, Gordon M. Shepherd, and Michael L. Hines. Twenty years of ModelDB and beyond: building essential modeling tools for the future of neuroscience. *Journal of Computational Neuroscience*, 42(1):1–10, February 2017.
- [32] C. Daniel Meliza, Mark Kostuk, Hao Huang, Alain Nogaret, Daniel Margoliash, and Henry D. I. Abarbanel. Estimating parameters and predicting membrane voltages with conductance-based neuron models. *Biological Cybernetics*, 108(4):495–516, August 2014.
- [33] Ekaterina Morozova, Peter Newstein, and Eve Marder. Reciprocally inhibitory circuits operating with distinct mechanisms are differently robust to perturbation and modulation. *eLife*, 11:e74363, February 2022.
- [34] Vignesh Narayanan, Jr-Shin Li, and ShiNung Ching. Biophysically interpretable inference of single neuron dynamics. *Journal of Computational Neuroscience*, 47(1):61–76, August 2019.
- [35] Luis Fernando Nicolas-Alonso and Jaime Gomez-Gil. Brain Computer Interfaces, a Review. *Sensors*, 12(2):1211–1279, January 2012.
- [36] Alain Nogaret, C. Daniel Meliza, Daniel Margoliash, and Henry D. I. Abarbanel. Automatic Construction of Predictive Neuron Models through Large Scale Assimilation of Electrophysiological Data. *Scientific Reports*, 6:32749, September 2016.
- [37] Razvan Pascanu, Tomas Mikolov, and Yoshua Bengio. On the difficulty of training recurrent neural networks. In *Proceedings of the 30th International Conference on Machine Learning*, volume 28 of *ICML’13*, pages 1310–1318, Atlanta, GA, USA, June 2013.
- [38] Marco Pengov, Edouard Richard, and Jean-Claude Vivalda. On the boundedness of the solutions of the continuous Riccati equation. *Journal of Inequalities and Applications*, 6(6):641–649, 2001.
- [39] Antônio H. Ribeiro, Koen Tiels, Jack Umenberger, Thomas B. Schön, and Luis A. Aguirre. On the smoothness of nonlinear system identification. *Automatica*, 121:109158, November 2020.
- [40] Shankar Sastry and Marc Bodson. *Adaptive control: stability, convergence, and robustness*. Dover Publications, Mineola, N.Y, 2011.
- [41] Raphael Schmetterling, Thiago B. Burghi, and Rodolphe Sepulchre. Adaptive conductance control. *Annual Reviews in Control*, August 2022.
- [42] R. Sepulchre, G. Drion, and A. Franci. Control Across Scales by Positive and Negative Feedback. *Annual Review of Control, Robotics, and Autonomous Systems*, 2(1):89–113, 2019.
- [43] A. A. Sharp, M. B. O’Neil, L. F. Abbott, and E. Marder. Dynamic clamp: computer-generated conductances in real neurons. *Journal of Neurophysiology*, 69(3):992–995, March 1993.
- [44] Ethan Sorrell, Michael E. Rule, and Timothy O’Leary. Brain–Machine Interfaces: Closed-Loop Control in an Adaptive System. *Annual Review of Control, Robotics, and Autonomous Systems*, 4(1):167–189, May 2021.
- [45] Karl Johan Åström and Björn Wittenmark. *Adaptive Control*. Dover Publications, Mineola, NY, 2nd edition, January 2008.
- [46] Hiroyasu Tsukamoto, Soon-Jo Chung, and Jean-Jacques Slotine. Learning-based Adaptive Control via Contraction Theory. *arXiv:2103.02987 [cs, eess, math]*, March 2021.
- [47] I. Y. Tyukin, D. V. Prokhorov, and C. van Leeuwen. Adaptation and Parameter Estimation in Systems With Unstable Target Dynamics and Nonlinear Parametrization. *IEEE Transactions on Automatic Control*, 52(9):1543–1559, September 2007.
- [48] Ivan Y. Tyukin, Erik Steur, Henk Nijmeijer, and Cees van Leeuwen. Adaptive observers and parameter estimation for a class of systems nonlinear in the parameters. *Automatica*, 49(8):2409–2423, August 2013.
- [49] Wei Wang and Jean-Jacques E. Slotine. On partial contraction analysis for coupled nonlinear oscillators. *Biological Cybernetics*, 92(1):38–53, December 2004.
- [50] Rafael Yuste, Jason N. MacLean, Jeffrey Smith, and Anders Lansner. The cortex as a central pattern generator. *Nature Reviews Neuroscience*, 6(6):477–483, June 2005.

- [51] Qinghua Zhang and A. Clavel. Adaptive observer with exponential forgetting factor for linear time varying systems. In *40th IEEE Conference on Decision and Control*, pages 3886–3891, Orlando, FL, USA, December 2001.



Thiago B. Burghi is a post-doctoral researcher in the Control Group of the Department of Engineering at the University of Cambridge. He received the Diplôme d'Ingénieur from ENSTA ParisTech, France, in 2012, and the B.Sc and M.Sc in Control Engineering and Mechanical Engineering, respectively, from the University of Campinas, Brazil, in 2015. He also holds a M.Sc in Robotics from the Pierre and Marie Curie University (Paris VI), France. Thiago was awarded the Capes-Cambridge Trust Scholarship to study

at the University of Cambridge, UK, where he completed his Ph.D in 2020. His research interests lie at the interface between nonlinear control theory, system identification, and biophysical neuronal systems.



Rodolphe Sepulchre (M96,SM08,F10) received the engineering degree and the Ph.D. degree from the Université Catholique de Louvain in 1990 and in 1994, respectively. He is Professor of Engineering at the University of Cambridge since 2013. His research interests are in nonlinear control and optimization, and more recently neuromorphic control. He co-authored the monographs "Constructive Nonlinear Control" (Springer-Verlag, 1997) and "Optimization on Matrix Manifolds" (Princeton

University Press, 2008). He is Editor-in-Chief of IEEE Control Systems. He is a recipient of the IEEE CSS Antonio Ruberti Young Researcher Prize (2008) and of the IEEE CSS George S. Axelby Outstanding Paper Award (2020). He is a fellow of IEEE, IFAC, and SIAM. He has been IEEE CSS distinguished lecturer between 2010 and 2015. In 2013, he was elected at the Royal Academy of Belgium.